

# Novel 3-Trifluoromethyl-1,2,4-oxadiazole Analogues of Astemizole with Multi-stage Antiplasmodium Activity and *In Vivo* Efficacy in a *Plasmodium berghei* Mouse Malaria Infection Model

Dickson Mambwe, Constance M. Korkor, Amanda Mabhula, Zama Ngqumba, Cleavon Cloete, Malkeet Kumar, Paula Ladeia Barros, Meta Leshabane, Dina Coertzen, Dale Taylor, Liezl Gibhard, Mathew Njoroge, Nina Lawrence, Janette Reader, Diogo Rodrigo Moreira, Lyn-Marie Birkholtz, Sergio Wittlin, Timothy J. Egan, and Kelly Chibale\*



Cite This: *J. Med. Chem.* 2022, 65, 16695–16715



Read Online

ACCESS |



Metrics & More

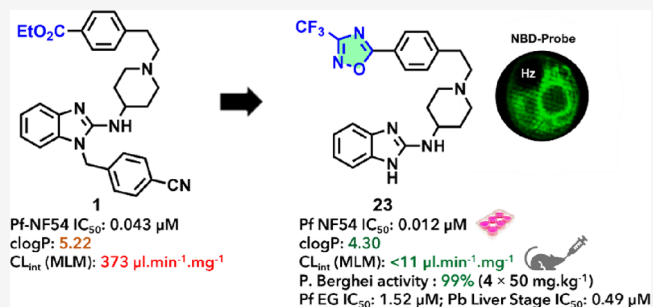


Article Recommendations



Supporting Information

**ABSTRACT:** Iterative medicinal chemistry optimization of an ester-containing astemizole (AST) analogue **1** with an associated metabolic instability liability led to the identification of a highly potent 3-trifluoromethyl-1,2,4-oxadiazole analogue **23** (*Pf*NF54  $IC_{50}$  = 0.012  $\mu$ M; *Pf*K1  $IC_{50}$  = 0.040  $\mu$ M) displaying high microsomal metabolic stability (HLM  $CL_{int}$  < 11.6  $\mu$ L $\cdot$ min $^{-1}$  $\cdot$ mg $^{-1}$ ) and > 1000-fold higher selectivity over hERG compared to AST. In addition to asexual blood stage activity, the compound also shows activity against liver and gametocyte life cycle stages and demonstrates *in vivo* efficacy in *Plasmodium berghei*-infected mice at 4  $\times$  50 mg $\cdot$ kg $^{-1}$  oral dose. Preliminary interrogation of the mode of action using live-cell microscopy and cellular heme speciation revealed that **23** could be affecting multiple processes in the parasitic digestive vacuole, with the possibility of a novel target at play in the organelles associated with it.



resistance to existing medicines to contribute to the pipeline of drugs under development is therefore imperative.

## INTRODUCTION

Malaria is a life-threatening infectious disease, affecting almost half of the world's population. It is caused by *Plasmodium falciparum* (*P. falciparum*, *Pf*) parasites and transmitted to humans by the female *Anopheles* mosquito.<sup>1</sup> Approximately 241 million global cases of malaria were recorded in 2020, with a mortality of 627,000. The Sub-Saharan Africa region accounted for 96% of total reported deaths,<sup>2</sup> and children under the age of 5 years were still among the most vulnerable groups. Notably, a steady decline in the global malaria mortality has been recorded between the year 2000 and 2019. This has been achieved through malaria elimination and prevention programs, increased investments in malaria research, improved diagnostic tools, and treatment among other malaria control initiatives.<sup>2</sup> However, malaria service disruptions during the COVID-19 pandemic resulted in a 12% rise in malaria deaths in 2020 compared to 2019.<sup>2</sup>

To date, the first line of treatment has been the effective artemisinin-based combination therapies (ACTs). However, reports of the emergence of resistance toward ACTs have continued to rise in Western Cambodia to the Greater Mekong Subregion and Africa, posing a serious threat to the global management and control of malaria.<sup>3,4</sup> The development of novel, pan active, and affordable chemotherapies with no cross-

resistance to existing medicines to contribute to the pipeline of drugs under development is therefore imperative.

Astemizole (AST, **Figure 1**) is a well-known second-generation antihistamine. However, it was withdrawn from the market in most countries due to its rare but fatal side effect implicated by QTc prolongation, torsades de pointes, cardiac arrhythmia due to hERG K<sup>+</sup> channel blockade.<sup>5,6</sup> AST and its principle metabolite desmethylastemizole (DMAST, **Figure 1**) were first identified to possess antimalarial properties by Chong and co-workers.<sup>7</sup>

Medicinal chemistry efforts aimed at addressing the hERG liability and optimizing antimalarial activity have previously been undertaken by a few groups and us. Musonda and co-workers demonstrated the potential to overcome *Pf* resistance to chloroquine (CQ) via a CQ-AST hybridization approach and identified hybrids (i.e., CCM-07, **Figure 1**) with high *in vivo* efficacy in the *P. berghei* (*Pb*) mouse infection model of malaria (99% activity at 4  $\times$  50 mg $\cdot$ kg $^{-1}$ ).<sup>8</sup> Furthermore,

Received: September 15, 2022

Published: December 12, 2022



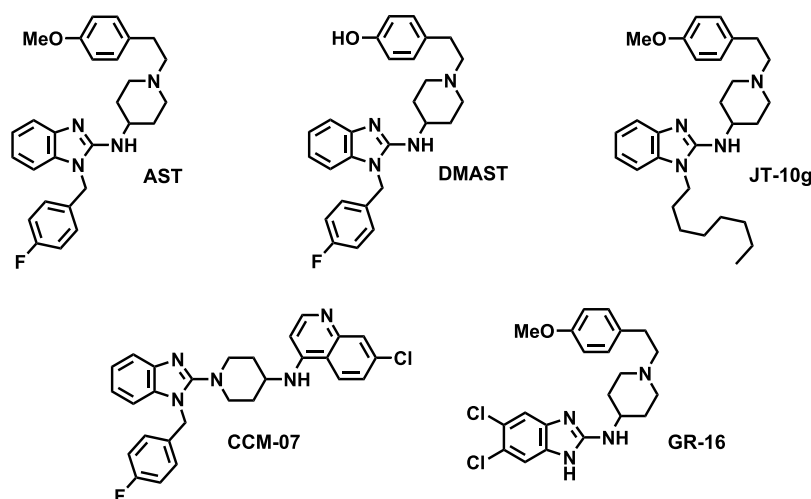


**Figure 1.** Chemical structures of astemizole (AST), desmethyastemizole (DMAST), and front-runner AST derivatives from the literature.

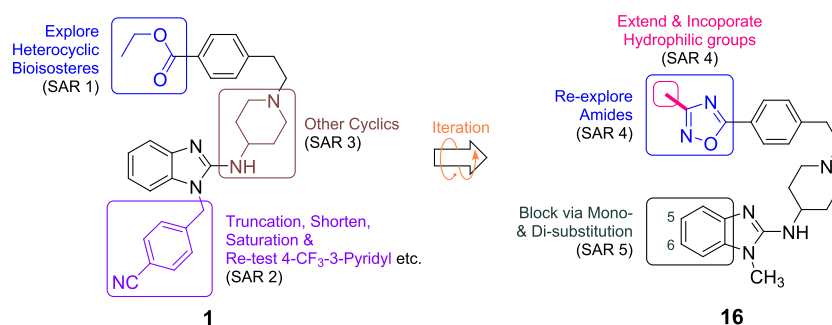


**Figure 2.** Progressive SAR design toward improving metabolic stability of compound 1.

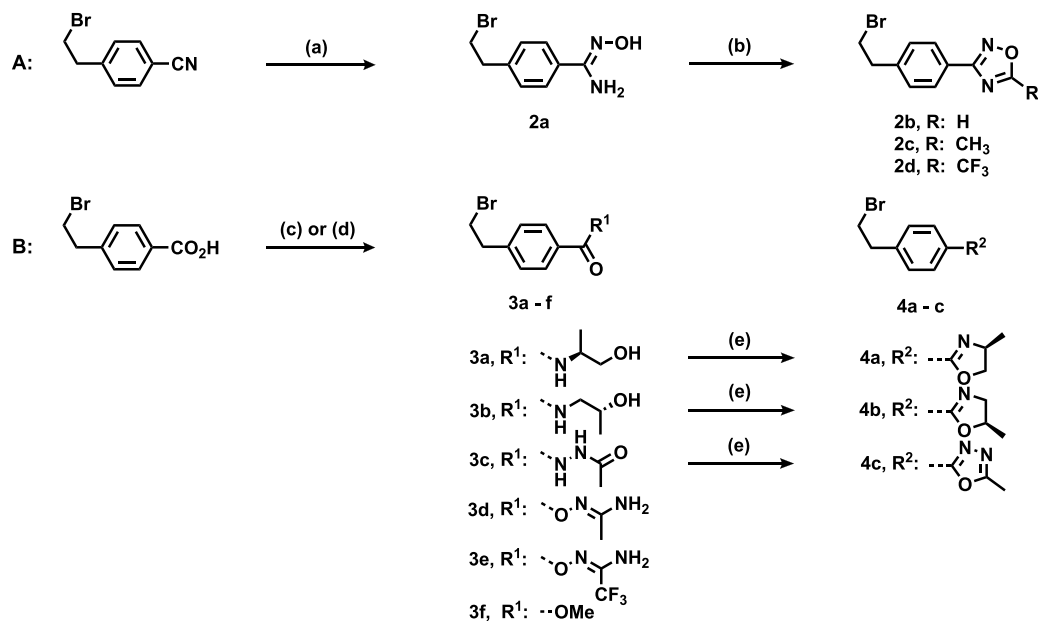
Roman and co-workers<sup>9</sup> and De Jonghe and co-workers<sup>10</sup> separately revealed crucial antiparasmodium structure–activity relationships (SAR) of AST. The former group identified highly active AST analogues such as **GR-16** (*Pf*ItG  $IC_{50}$  = 0.083  $\mu$ M) with a truncated 4-F-benzyl group and a 5,6-dichloro substitution in the benzimidazole core (Figure 1). On the other hand, De Jonghe *et al.* revealed a potent AST analogue **JT-10g** (*Pf*3D7  $IC_{50}$  = 0.030  $\mu$ M) with reduced hERG channel inhibitory activity (hERG  $IC_{50}$  = 0.030  $\mu$ M; SI = 110, Figure 3). However, the poor drug-likeness characterized by high lipophilicity and poor solubility of analogues such as **JT-10g** would present development challenges.

To build on this work, our group initiated a project aimed at repositioning AST by expanding the existing antiparasmodium SAR around AST and improving drug-like properties. Initially, we reported AST analogues with improved potency, enhanced solubility, and potential for multi-stage activity against asexual blood stages (*ABS*, *Pf*NF54  $IC_{50}$ s = 0.033–1.9  $\mu$ M), liver stages (*Pb*  $IC_{50}$  = 0.210  $\mu$ M), and late-stage gametocytes (stage IV/V; *Pf*LG  $IC_{50}$ s = 1.9–4.1  $\mu$ M).<sup>11</sup> Furthermore, our work implicated intracellular inhibition of hemozoin formation by these analogues within the parasite as a contributing mode of action, which supported previous findings of interference of AST with the heme detoxification pathway.<sup>7,11</sup> With the exception of the hybridization work reported by Musonda and co-workers,<sup>8</sup> all studies so far have not progressed any analogues to proof-of-concept (PoC) *in vivo* efficacy studies. Herein, we report SAR studies and a multi-parameter optimization campaign that led to the discovery of novel structural analogues of AST with *in vivo* PoC in mice and

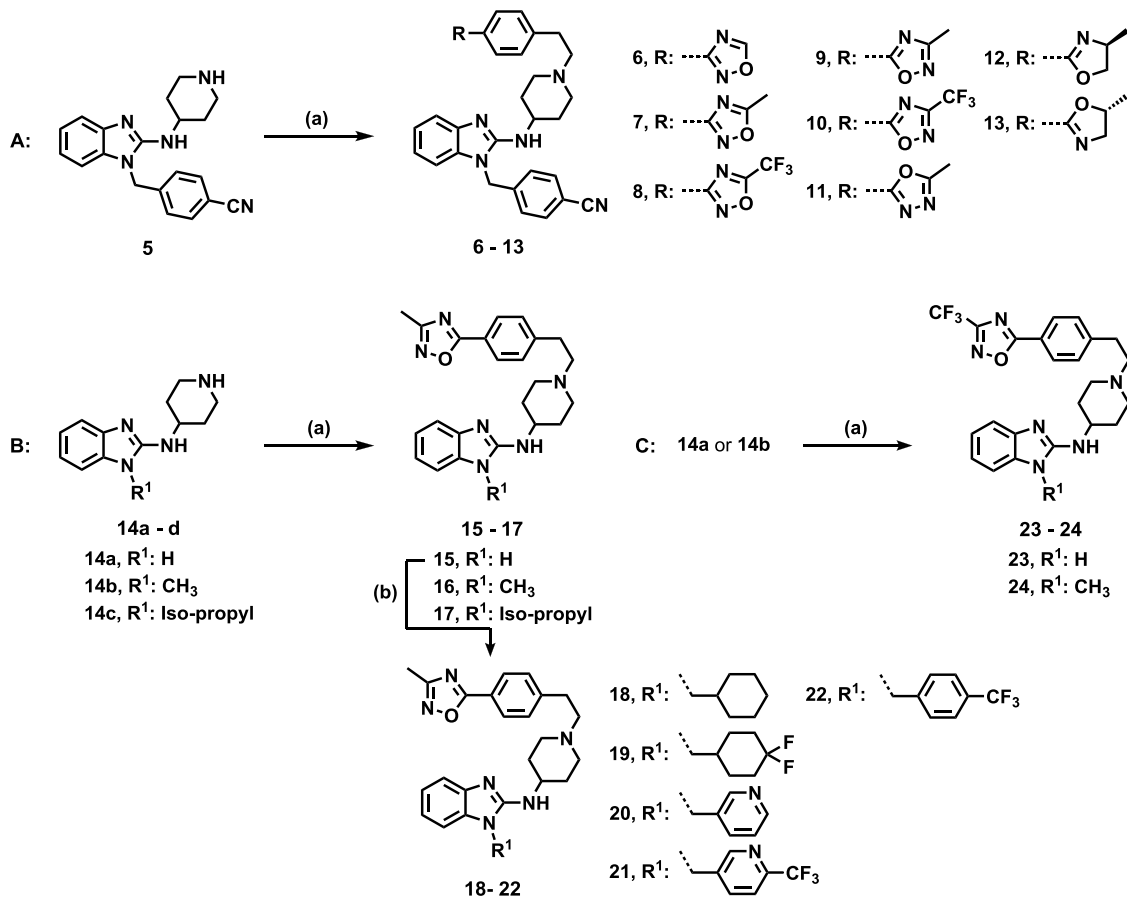
mechanistic insights using live-cell microscopy, providing significant advances over previous studies.

An ester-containing AST analogue **1** (Figure 2) emerged with high *in vitro* *Pf* activity and favorable solubility from our recent work; however, and unsurprisingly, it had poor microsomal metabolic stability.<sup>12</sup> This prompted an optimization campaign to improve microsomal metabolic stability toward identifying an AST analogue for PoC studies. While various strategies are known to address the metabolic liability associated with the ester group, bioisosterism is one of the most common approaches for hydrolysis-labile groups such as esters.<sup>13</sup> In this regard, we focused on ring replacements for the ethyl ester group in compound **1**, particularly exploring five-membered heterocycles to maintain spatial geometry and increase structural rigidity (Figure 2, SAR 1).<sup>14,15</sup> Following the identification and fixing of a more stable ester surrogate in SAR 1, we then sought to explore other parts of the molecule in an effort to enhance potency and solubility as well as to further reduce hERG affinity, and deliver a compound for *in vivo* efficacy studies.

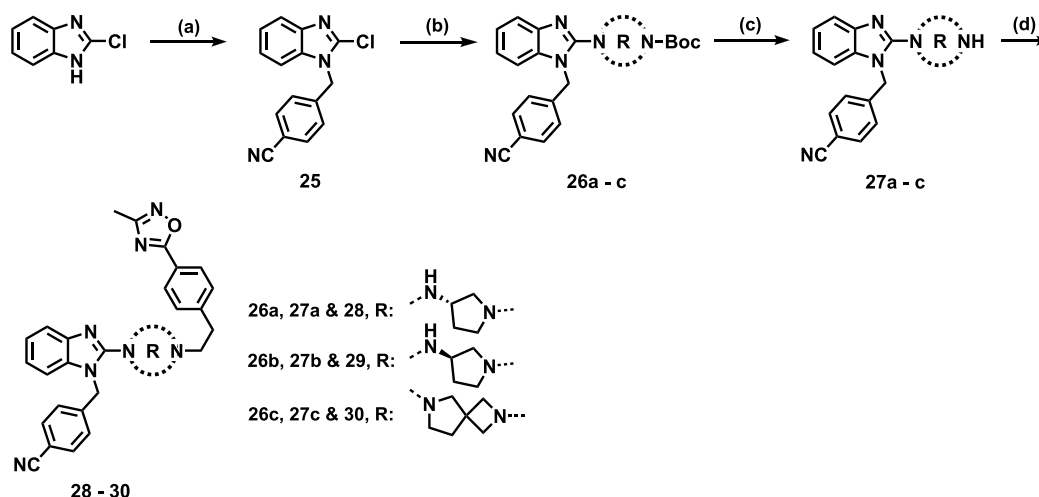
In SAR 2, we revisited the previously explored SAR around the benzyl moiety, but this time to include ring saturation (Figure 2). In SAR 3, the 4-aminopiperidine linker was replaced with other cyclics not previously explored. Based on learnings from SARs 1–3, we iteratively replaced the 4-CN-benzyl group with *N*-methyl and explored the SAR at the 3-position of the 1,2,4-oxadiazole moiety, including replacement with various amides (SAR 4, Figure 2). CYP-mediated hydroxylation of DMAST at benzimidazole position 6 is known to generate the 6-hydroxydesmethyastemizole (6-OH-

Scheme 1. Synthetic Approach for Intermediates 2–4<sup>a</sup>

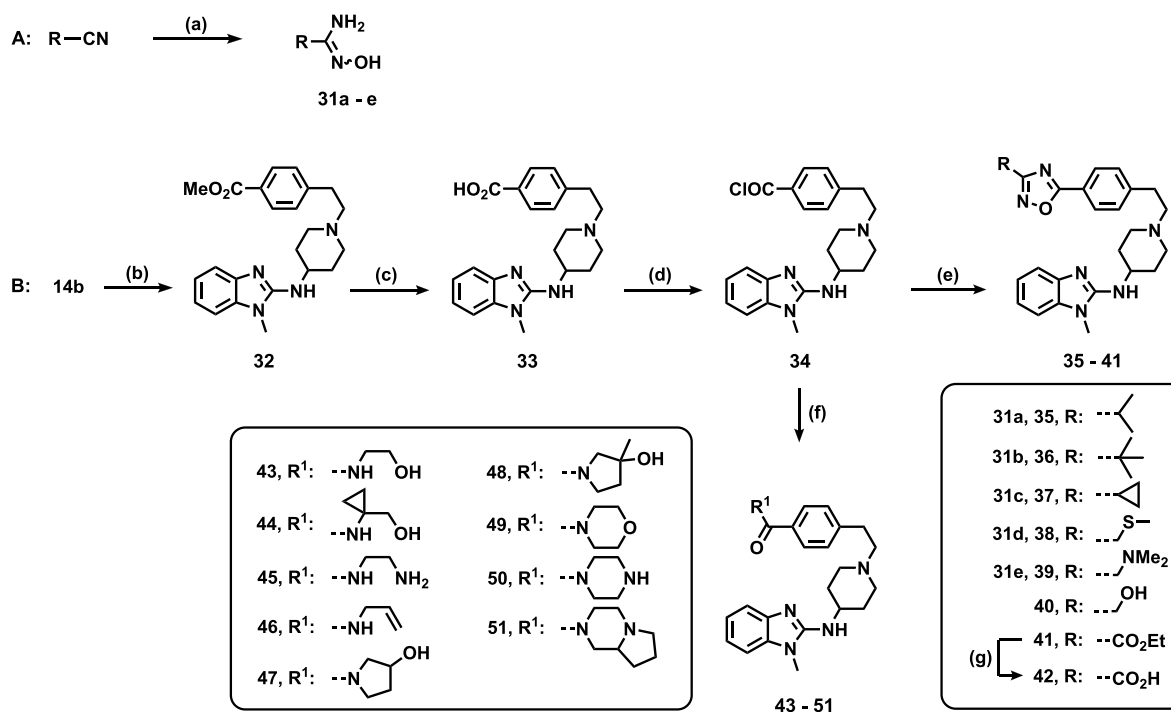
<sup>a</sup>Reagents and conditions: (a) (i) NH<sub>2</sub>OH·HCl, 8-hydroxyquinolone, Et<sub>3</sub>N, EtOH, 79 °C, 1.5 h, (ii) 21 °C, 10% HCl, pH 3 (82%); (b) for 2b: CH(EtO)<sub>3</sub>, BF<sub>3</sub>·OEt<sub>2</sub>, pyridine, 80 °C, 1 h (51%); for 2c: acetyl chloride, 50 °C, 0.5 h (80%); for 2d: (CF<sub>3</sub>CO)<sub>2</sub>O, DCM, pyridine, 21 °C, 20 min (76%); (c) amine or amidoxime, EDCl, DMAP, DCM, 18 °C, 2 h (65–91%); (d) TMS-CHN<sub>2</sub>, MeOH, toluene, 21 °C, 0.5 h (3f, 97%); (e) TsCl, Et<sub>3</sub>N, DCM, 30 °C, 0.5 h (4a, 70%; 4b, 85%; 4c, 88%).

Scheme 2. Synthetic Approach for Analogues 6–25 (SARs 1 and 2)<sup>a</sup>

<sup>a</sup>Reagents and conditions: (a) phenethyl bromide (2b–d, 3d,e, or 4a–c), K<sub>2</sub>CO<sub>3</sub>, 80 °C, 5–12 h (48–91%); (b) alkyl bromide, K<sub>2</sub>CO<sub>3</sub>, DMF, 70 °C, 12 h (58–80%).

Scheme 3. Synthetic Approach for Analogues 28–30 (SAR 3)<sup>a</sup>

<sup>a</sup>Reagents and conditions: (a) 4-(bromomethyl)benzotrile,  $K_2CO_3$ , acetone, 23 °C, 2 h (98%); (b) *N*-Boc-amine,  $Et_3N$ , toluene, 150 °C,  $\mu W$ , 5–30 min (55–78%); (c) TFA, DCM, 23 °C, 2 h (75–98%); (d) **3d**,  $K_2CO_3$ , 80 °C, 10–24 h (67–80%).

Scheme 4. (A, B) Synthetic Approach for Analogues 35–50 (SAR 4)<sup>a</sup>

<sup>a</sup>Reagents and conditions: (a)  $NH_2OH \cdot HCl$ , 8-hydroxyquinolone,  $Et_3N$ , ethanol, 79 °C, 2 h, (70–95%); (b) **3f**,  $K_2CO_3$ , 80 °C, 5 h (68%); (c) 2 M NaOH, MeOH, 78 °C, 2 h, then 3 N HCl, pH 2, 20 °C (98%); (d)  $SOCl_2$ , 80 °C, 2 h (99%); (e) (i) amidoxime,  $Et_3N$ , dry THF, 20 °C, 2–10 h; (ii)  $K_2CO_3$ , MeCN, 85 °C, 16 h (44–60% over two steps); (f) amine,  $Et_3N$ , dry THF, 23 °C, 6–10 h (66–98%); (g) 2 N NaOH, EtOH, 80 °C, 2 h; then 3 N HCl, pH 2, 20 °C (96%).

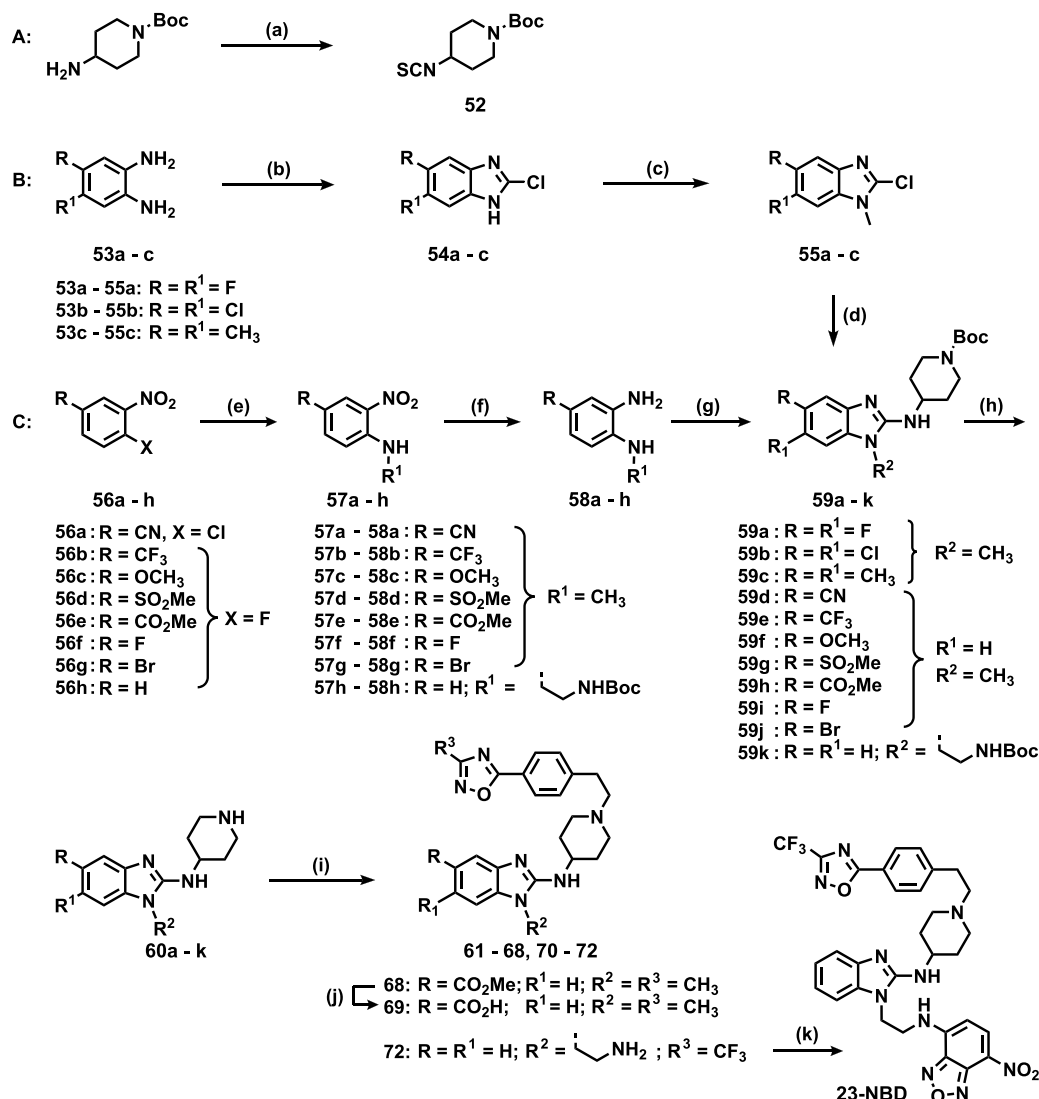
DMAST) metabolite *in vivo*, thereby contributing to the clearance of AST and DMAST.<sup>5</sup> For this reason, we sought to either block or sterically hinder the 6-benzimidazole position by exploring various substituents at both positions 5 and 6 (SAR 5, Figure 2).

## CHEMISTRY

The synthesis of target compounds commenced with the preparation of various phenethyl bromide intermediates (2–4) using modified literature methods (Scheme 1).<sup>16–20</sup>

Analogues 6–13 (SAR 1, Scheme 2) and 15–24 (SAR 2, Scheme 2) were synthesized by coupling phenethyl bromides 2–4 or commercially sourced alkylating agents to previously reported amine intermediates 5 and 14a,b, respectively (Scheme 1).<sup>12</sup> Compound 17 was prepared from isopropyl intermediate 14c, which had been synthesized following previously reported synthetic procedures.<sup>12</sup>

Coupling of 2-chlorobenzimidazole and 4-(bromomethyl)-benzotrile followed by microwave-assisted nucleophilic aromatic substitution ( $S_NAr$ ) with a series of commercially

Scheme 5. (A–C) Synthetic Approach for Analogues 61–71 & 23-NBD (SAR 5)<sup>a</sup>

<sup>a</sup>Reagents and conditions: (a) 1,1-thiocarbonyldiimidazole, DMF, 23 °C, 12 h (97%); (b) (i) CDI, DMAP, THF, 20 °C, 12 h (quant); (ii) POCl<sub>3</sub>, 110 °C, 12 h (58–93%); (c) CH<sub>3</sub>I, acetone, K<sub>2</sub>CO<sub>3</sub>, 23 °C, 2 h (90–97%); (d) *tert*-butyl 4-aminopiperidine-1-carboxylate, Et<sub>3</sub>N, 150 °C, 2–12 h (66–85%); (e) 2 M CH<sub>3</sub>NH<sub>2</sub> in THF (for 57a–g) or *N*-Boc-ethylenediamine (for 57h), Et<sub>3</sub>N, MeCN, 65 °C, 4–18 h, (66–96%); (f) H<sub>2</sub>, balloon, 10% Pd/C, 1:1 MeOH/EtOAc, 21 °C, 12 h (89–96%); (g) 52, DCC, TEA, MeCN, 85 °C, 12 h (80–95%); (h) TFA, DCM, 21 °C, 3 h (71–98%); (i) 3d (for 61–71) or 3e (for 72), MeCN, 85 °C, 8–12 h (46–78%); (j) 2 M NaOH, EtOH, 25 °C, 12 h; then 3 N aq. HCl, pH 2, 20 °C (94%); (k) 4-chloro-7-nitrobenzoxadiazole, NaHCO<sub>3</sub>, 1:1 MeCN/H<sub>2</sub>O, 65 °C, 12 h (68%).

sourced mono-*N*-Boc-protected diamines produced intermediates 26 in good yields (Scheme 3). *N*-Boc deprotection of 26 resulted in free amine intermediates 27, which were subjected to a final *N*-alkylation step with 3d to afford analogues 28–30 in high yields.

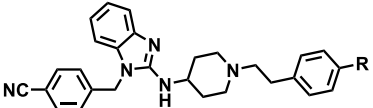
In SAR 4 (Scheme 4), various amidoximes (31) were initially prepared from the respective nitriles using hydroxylamine hydrochloride in EtOH (Scheme 4A). Second, a nucleophilic substitution reaction between 14b and 3f afforded ester 32, which was hydrolyzed to 33, followed by treatment with thionyl chloride to give acyl chloride 34, quantitatively. Amidoximes (31) and amines were coupled to 34 in the presence of Et<sub>3</sub>N to produce *O*-acyl amidoximes and amides (43–51), respectively. The 3-substituted-1,2,4-oxadiazoles (35–41) were directly obtained from the respective *O*-acyl amidoximes via K<sub>2</sub>CO<sub>3</sub>-mediated cyclo-condensation in

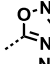
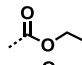
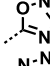
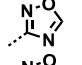
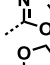
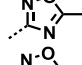
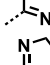
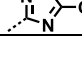
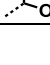
MeCN at 85 °C, while acid 42 was prepared from hydrolysis of ester 41 (Scheme 4B).

SAR 5 analogues were prepared via two converging synthetic routes (Scheme 5B,C) to access 5,6-disubstituted and 5-substituted benzimidazole analogues. For 5,6-disubstituted analogues, cyclization of commercially sourced 4,5-disubstituted-1,2-diamines (53a–c) with 1,1-carbonyldiimidazole (CDI) followed by chlorination using POCl<sub>3</sub> produced corresponding 5,6-disubstituted-2-chloro-1*H*-benzimidazoles 54a–c.

*N*-Methylation of 54a–c using methyl iodide afforded 5,6-disubstituted-1-methyl-2-chlorobenzimidazoles 55a–c, which were subjected to S<sub>N</sub>Ar coupling with *N*-Boc-4-aminopiperidine in Et<sub>3</sub>N at 150 °C, to give 59a–c in good yields (Scheme 5B).

On the other hand, preparation of 5-substituted analogues was initiated by S<sub>N</sub>Ar reaction between methylamine (2 M in

Table 1. *In Vitro* Antiplasmodium Activity and Solubility of SAR 1 Analogues


Compound	R	$PfIC_{50}$ ( $\mu\text{M}$ ) <sup>a</sup>		RI <sup>b</sup>	Sol. <sup>c</sup> ( $\mu\text{M}$ )	Compound	R	$PfIC_{50}$ ( $\mu\text{M}$ ) <sup>a</sup>		RI <sup>b</sup>	Sol. <sup>c</sup> ( $\mu\text{M}$ )
		NF54	K1					NF54	K1		
AST		0.086	0.370	4.3	40	9		0.097	0.178	1.8	20
1		0.043	0.052	1.2	40	10		0.022	0.027	1.2	10
6		0.089	0.399	4.5	40	11		0.519	ND	-	20
7		0.051	0.174	3.4	40	12		0.074	0.263	3.6	20
8		0.021	0.049	2.3	20	13		0.104	0.352	3.4	60
CQ		0.004	0.14	35	-						

<sup>a</sup>Mean from  $n \geq 2$  independent experiments with sensitive (NF54) and multidrug-resistant (K1) strains of *P. falciparum*. <sup>b</sup>Resistance index (RI) =  $[(PfK1 IC_{50})/(PfNF54 IC_{50})]$ . <sup>c</sup>Turbidimetric kinetic solubility at pH 7.4; ND = not determined; CQ = chloroquine.

THF) or *N*-Boc-ethylenediamine and an appropriately substituted *o*-halo-nitrobenzene (**56a–h**) in the presence of  $\text{Et}_3\text{N}$  at 65 °C in MeCN (Scheme 5). The resulting 1-amino-2-nitrobenzenes (**57a–h**) were subjected to a reduction [ $\text{H}_2$ , Pd/C] step to afford 1,2-diamines **58a–h** in high yields (Scheme 5C). *N,N'*-Dicyclohexylcarbodiimide (DCC)-mediated cyclization of the diamines **58a–h** with previously prepared isothiocyanate **52** (Scheme 5A) in MeCN produced 2-amino benzimidazoles **59d–k** in moderate yields (48–79%). *N*-Boc deprotection of **59a–k** using TFA afforded free amines **60a–k**, which were subsequently coupled ( $\text{S}_{\text{N}}2$ ) with **3d** to afford the final compounds **61–68** and **70** and **71** in good yields. Carboxylic acid analogue **69** was obtained *via* hydrolysis of ester **68**, while 7-nitrobenzoxadiazole (NBD)-tagged fluorescent probe **23-NBD** was prepared *via*  $\text{S}_{\text{N}}\text{Ar}$  between corresponding amine **72** and 4-chloro-7-nitrobenzoxadiazole (NBD-Cl).

## RESULTS AND DISCUSSION

**In Vitro Asexual Blood Stage Antiplasmodium Activity and Solubility.** All target compounds were evaluated for their *in vitro* antiplasmodium activity (Table 1) against the drug-sensitive strain of *P. falciparum* NF54 ( $PfNF54$ ) and aqueous turbidimetric kinetic solubility at pH 7.4. Compounds that displayed high activity ( $IC_{50} < 0.20 \mu\text{M}$ ) in the sensitive strain ( $PfNF54$ ) were further screened against the multi-drug resistant (MDR) strain  $PfK1$ , to assess the potential of cross-resistance with existing antimalarial drugs (i.e., chloroquine).

**Bioisosteric Replacement of the Ester Group (SAR 1).** Heterocyclic 1,2,4-oxadiazole and oxazoline isosteres produced analogues with general retention of potency ( $PfNF54 IC_{50}$ s = 0.021–0.104  $\mu\text{M}$ , Table 1) relative to the ester compound (**1**,  $PfNF54 IC_{50}$ : 0.043  $\mu\text{M}$ ).

Interestingly, a  $\sim 2$ -fold increase in potency was consistently observed following the introduction of methyl (5- $\text{CH}_3$ , **7**,  $PfNF54 IC_{50}$  = 0.051  $\mu\text{M}$ ) and trifluoromethyl (5- $\text{CF}_3$ , **8**,  $PfNF54 IC_{50}$  = 0.021  $\mu\text{M}$ ) substituents relative to 5-unsubstituted 1,2,4-oxadiazole analogue **6** ( $IC_{50}$  = 0.089  $\mu\text{M}$ ). Similarly, reversed 3-substituted-1,2,4-oxadiazoles dis-

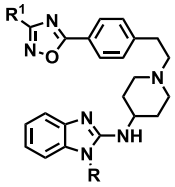
played a 4-fold potency difference between 3- $\text{CH}_3$  (**9**,  $PfNF54 IC_{50}$  = 0.097  $\mu\text{M}$ ) and 3- $\text{CF}_3$  (**10**,  $PfNF54 IC_{50}$  = 0.022  $\mu\text{M}$ ) analogues.

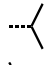
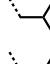


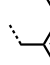
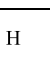
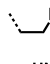

Compared to 1,2,4-oxadiazoles, activity was diminished by 12-fold in 1,3,4-oxadiazole analogue **11** ( $PfNF54 IC_{50}$  = 0.519  $\mu\text{M}$ , Table 1), an observation that may be attributed to the differences in the level of aromaticity between 1,2,4-oxadiazoles and 1,3,4-oxadiazoles. Being less aromatic, 1,2,4-oxadiazoles are more closely related to esters than 1,3,4-oxadiazole congeners are, and as a result, this potentially translates into differences in intrinsic biomacromolecule interactions between the two isomeric forms.<sup>21</sup> 4-Methyl-oxazoline **12** ( $PfNF54 IC_{50}$  = 0.074  $\mu\text{M}$ ) displayed comparable activity with the 5-methyl-oxazoline congener **13** ( $PfNF54 IC_{50}$  = 0.104  $\mu\text{M}$ ). All analogues from this SAR displayed low to moderate solubility (10–60  $\mu\text{M}$ ).

**Benzyl Group and Diamine Linker (SARs 2 and 3).** Next, we retained the 3- $\text{CH}_3$ -1,2,4-oxadiazole ring (**9**) and re-explored the SAR at the benzimidazole *N*-1 position (Table 2). Consistently, activity was retained following replacement of the 4-CN-benzyl group with 4- $\text{CF}_3$ -containing aromatic moieties (**21**,  $PfNF54 IC_{50}$  = 0.044  $\mu\text{M}$  and **22**,  $PfNF54 IC_{50}$  = 0.030  $\mu\text{M}$ ) and saturated (cyclohexyl)methyl (**18**,  $PfNF54 IC_{50}$  = 0.093  $\mu\text{M}$ , Table 2).

Interestingly, the *N*-methyl analogue (**16**,  $PfNF54 IC_{50}$  = 0.033  $\mu\text{M}$ ) and truncation of the benzyl group (**15**,  $PfNF54 IC_{50}$  = 0.055  $\mu\text{M}$ ) produced compounds with high activity and high solubility (>80  $\mu\text{M}$ ). Previously, this change drastically reduced activity in analogues containing a cyano (CN) group in place of the oxadiazole ring.<sup>12</sup>

Conversely, isopropyl (**17**) and (4,4-difluorocyclohexyl)-methyl (**19**) analogues displayed reduced activities (Table 2) and low solubility (20  $\mu\text{M}$ ). Inspired by the identification of compounds **15** and **16**, and the consistently observed superior activity of 3-/5- $\text{CF}_3$ -containing 1,2,4-oxadiazole analogues (**8** and **10**) over 3-/5- $\text{CH}_3$ -containing match pairs we synthesized compounds **23** and **24**. Gratifyingly, **23** demonstrated a significant (4.6-fold) increase in potency ( $PfNF54 IC_{50}$  = 0.012  $\mu\text{M}$ ) compared to **15**, while a 2-fold potency drop was

**Table 2.** *In Vitro* Antiplasmodium Activity and Solubility of SAR 2 Analogues and NBD-Probe 72


Compound	R	R <sup>1</sup>	<i>Pf</i> IC <sub>50</sub> (μM) <sup>a</sup>		RI <sup>b</sup>	Sol. <sup>c</sup> (μM)
			NF54	K1		
15	H		0.055	0.176	3.2	80
16	CH <sub>3</sub>		0.033	0.082	2.5	160
17			0.702	-	-	20
18			0.093	0.156	1.7	80
19		CH <sub>3</sub>	0.460	-	-	20
20			0.304	-	-	ND
21			0.044	0.173	3.9	40
22			0.030	0.104	3.5	10
23	H		0.012	0.040	3.3	100
24	CH <sub>3</sub>		0.066	0.048	0.7	160
71 <sup>d</sup>		CF <sub>3</sub>	0.090	0.036	0.40	>200
23-NBD <sup>d</sup>			0.140	0.370	2.64	120
CQ			0.004	0.14	35.0	-

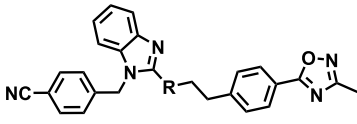
<sup>a</sup>Mean from  $n \geq 2$  independent experiments with sensitive (NF54) and multidrug-resistant (K1) strains of *P. falciparum*. <sup>b</sup>Resistance index (RI) = [(*Pf*K1 IC<sub>50</sub>)/(*Pf*NF54 IC<sub>50</sub>)]. <sup>c</sup>Turbidimetric kinetic solubility at pH 7.4. <sup>d</sup>Tested at Swiss TPH using the 72 h [<sup>3</sup>H] hypoxanthine incorporation assay; ND = not determined; CQ = chloroquine.

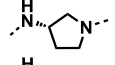
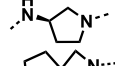
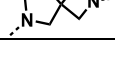
observed in **24** (*Pf*NF54 IC<sub>50</sub> = 0.066 μM) relative to **16**, albeit maintaining high solubility profiles (160 μM).

Using **9** as the benchmark, we next re-explored the 4-aminopiperidine linker SAR by replacing it with (*R*)- and (*S*)-3-amino pyrrolidine and 2,6-diazaspiro[3.4]octane (**28–29**, Table 3). All three analogues had comparable activities (**28–30**, Table 3), albeit ~5-fold lower compared to **9**. Additionally, all analogues in this SAR showed low to moderate solubility (40–80 μM).

**Exploring the 3-Position of the 1,2,4-Oxadiazole Moiety and Amidation (SAR 4).** In this SAR, compound **16** was iteratively used as a template to derive further analogues. We envisaged that *N*-methyl-containing analogues would possess lower molecular weight, aromatic character, and lipophilicity (clog*P*), which would potentially translate into favorable solubilities and reduced hERG channel inhibition.

Functionalization of the 1,2,4-oxadiazole moiety at the 3-position by introducing both alkyl and polar atom (group)-containing moieties produced analogues with up to >15-fold lower activity (**35**, *Pf*NF54 IC<sub>50</sub> = 0.492 μM, Table 4)

**Table 3.** *In Vitro* Antiplasmodium Activity and Solubility of SAR 3 Analogues


Compound	R	<i>Pf</i> NF54 IC <sub>50</sub> (μM) <sup>a</sup>	Sol. <sup>c</sup> (μM)
28		0.515	80
29		0.448	80
30		0.446	40
CQ		0.004	-

<sup>a</sup>Mean from  $n \geq 2$  independent experiments with sensitive (NF54) and multidrug-resistant (K1) strains of *P. falciparum*. <sup>b</sup>Turbidimetric kinetic solubility at pH 7.4; ND = not determined; CQ = chloroquine.

compared to **16**. However, the *tert*-butyl analogue **36** (*Pf*NF54 IC<sub>50</sub> = 0.064 μM) retained high activity and was equipotent to **24** (*Pf*NF54 IC<sub>50</sub> = 0.066 μM). This is not entirely surprising as the *tert*-butyl group has been widely used as an effective CF<sub>3</sub>-group surrogate. No apparent difference in activity was observed between cyclopropyl and isopropyl (**35** and **37**) groups, attributable to subtle steric differences between the two groups.<sup>22,23</sup> Incorporation of a carboxylic acid moiety at this position was detrimental to activity (**42**, *Pf*NF54 IC<sub>50</sub> > 6.0 μM, Table 4), a consistent trend observed for all carboxylic acid-containing analogues of AST (i.e., **33**). Solubility was consistently lower in analogues containing alkyl groups compared to those with polar atoms.

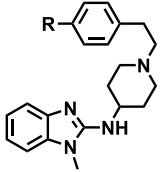
All amides displayed low antiplasmodium activities (**43–51**, *Pf*NF54 IC<sub>50</sub> > 1.70 μM), with an unclearly discernable antiplasmodium SAR within the set of analogues prepared (Table 4). Coupled with the observed high activity derived from analogues **15** and **16**, this suggested the apparent existence of SAR between the presence (or absence) of the benzyl group at *N*-1, relative to an appropriate functionality at the 4-position of the lateral phenyl group. All amides exhibited moderate to high solubility (60–180 μM).

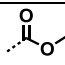
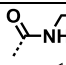
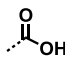
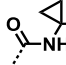
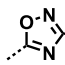
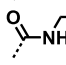
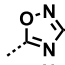
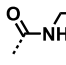
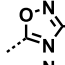
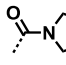
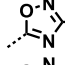
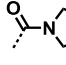
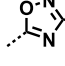
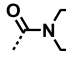
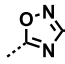
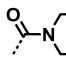
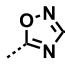
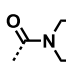
**Benzimidazole Ring Substitution (SAR 5).** We next investigated substitution of the benzimidazole ring at positions 5 and 6 in front-runner **16**. Activity was generally diminished across the SAR (Table 5).

It is noteworthy that 5,6-dimethyl analogue **61** (*Pf*NF54 IC<sub>50</sub> = 0.163 μM) displayed the highest activity overall and in comparison with halogen match pairs 5,6-F **62** (*Pf*NF54 IC<sub>50</sub> = 1.16 μM) and 5,6-Cl **63** (*Pf*NF54 IC<sub>50</sub> = 0.514 μM). Chloro substitution was better tolerated than fluoro substitution, resulting in ~2-fold higher activity in both the mono- and disubstituted fluoro congeners (**70**, *Pf*NF54 IC<sub>50</sub> = 0.834 μM and **62**, *Pf*NF54 IC<sub>50</sub> = 1.161 μM). Consistently, activity was lost in carboxylic acid derivative **69** (*Pf*NF54 IC<sub>50</sub> > 6 μM) albeit displaying high solubility (sol. = 160 μM).

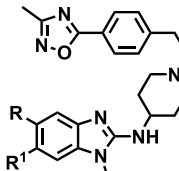
No potential for cross-resistance with existing antimalarial drugs was observed in analogues from this work based on the low resistance indices (RI < 5) with the *Pf*K1 strain (Tables 1, 2, and 4).

**Metabolic Stability.** Active compounds (*Pf*NF54-IC<sub>50</sub> < 0.10 μM) with moderate solubility (>20 μM) were evaluated

Table 4. *In Vitro* Antiplasmodium Activity and Solubility of SAR 4 Analogues


Compound	R	$PfIC_{50}$ ( $\mu\text{M}$ ) <sup>a</sup>		RI <sup>b</sup>	Sol. <sup>c</sup> ( $\mu\text{M}$ )	Compound	R	$PfNF54$ IC <sub>50</sub> ( $\mu\text{M}$ ) <sup>a</sup>	Sol. <sup>c</sup> ( $\mu\text{M}$ )
		NF54	K1						
32		1.450	-		120	43		4.170	120
33		>6	-		160	44		1.730	60
35		0.492	-		60	45		>6	100
36		0.064	0.30	4.6	60	46		2.610	80
37		0.484	-		60	47		3.990	80
38		0.383	-		80	48		>6	80
39		0.831	-		120	49		>6	80
40		0.567	-		100	50		3.410	120
42		>6	-		120	51		1.280	60
CQ		0.004	0.14	35	-				

<sup>a</sup>Mean from  $n \geq 2$  independent experiments with sensitive (NF54) and multidrug-resistant (K1) strains of *P. falciparum*. <sup>b</sup>Resistance index (RI) =  $[(PfK1 IC_{50})/(PfNF54 IC_{50})]$ . <sup>c</sup>Turbidimetric kinetic solubility at pH 7.4; ND = not determined; CQ = chloroquine.

Table 5. *In Vitro* Antiplasmodium Activity and Solubility of SAR 5 Analogues


somponent	R	R <sup>1</sup>	$PfNF54$ IC <sub>50</sub> ( $\mu\text{M}$ ) <sup>a</sup>	sol. <sup>c</sup> ( $\mu\text{M}$ )	compound	R	R <sup>1</sup>	$PfNF54$ IC <sub>50</sub> ( $\mu\text{M}$ ) <sup>a</sup>	sol. <sup>c</sup> ( $\mu\text{M}$ )
60	CH <sub>3</sub>	CH <sub>3</sub>	0.163	60	66	SO <sub>2</sub> Me	H	4.651	60
61	F	F	1.161	80	67	CO <sub>2</sub> Me		0.496	120
62	Cl	Cl	0.514	80	68	CO <sub>2</sub> H		>6	160
63	CN	H	0.611	80	69	F		0.834	80
64	CF <sub>3</sub>		0.422	40	70	Br		0.720	80
65	OMe		0.309	80	CQ <sup>f</sup>			0.004	

<sup>a</sup>Mean from  $n \geq 2$  independent experiments with sensitive (NF54) and multidrug-resistant (K1) strains of *P. falciparum*. <sup>b</sup>Resistance index (RI) =  $[(PfK1 IC_{50})/(PfNF54 IC_{50})]$ . <sup>c</sup>Turbidimetric kinetic solubility at pH 7.4; ND = not determined; CQ = chloroquine.

for their microsomal metabolic stability using mouse and human liver microsomes (MLM and HLM, Table 6).<sup>24</sup> Following the replacement of the labile ethyl ester (**1**, MLM CL<sub>int</sub> = 323  $\mu\text{L}\cdot\text{min}^{-1}\cdot\text{mg}^{-1}$ ) group with heterocyclic surrogates, the 3-unsubstituted 1,2,4-oxadiazole analogue **6** (MLM CL<sub>int</sub> = 266  $\mu\text{L}\cdot\text{min}^{-1}\cdot\text{mg}^{-1}$ ) still showed a high metabolic instability profile compared to 3-CH<sub>3</sub>-(**7**, MLM CL<sub>int</sub> = 67.4  $\mu\text{L}\cdot\text{min}^{-1}\cdot\text{mg}^{-1}$ ) and 3-CF<sub>3</sub>-(**8**, MLM CL<sub>int</sub> = 26.4  $\mu\text{L}\cdot\text{min}^{-1}\cdot\text{mg}^{-1}$ ) substituted match pairs in which the 3-position is blocked. Oxazoline derivative **12** (MLM CL<sub>int</sub> =

71.3  $\mu\text{L}\cdot\text{min}^{-1}\cdot\text{mg}^{-1}$ ) also showed marked improvement, albeit sub-optimal (MLM CL<sub>int</sub> > 12  $\mu\text{L}\cdot\text{min}^{-1}\cdot\text{mg}^{-1}$ ;  $\leq 95\%$  remaining) especially in the rodent strain (MLM) across the SAR. This was, however, circumvented following the truncation of the benzyl group and retaining the 3-CF<sub>3</sub>-1,2,4-oxadiazole moiety (**23** and **24**, MLM CL<sub>int</sub> < 11.6  $\mu\text{L}\cdot\text{min}^{-1}\cdot\text{mg}^{-1}$ ).

Unaided by metabolite identification experiments, this suggested that microsomal metabolism (i.e., phase I) also occurred in the benzyl moiety, in addition to the ester group in



**Table 6.** *In Vitro* Microsomal Metabolic Stability of Selected Analogues<sup>a</sup>

compound	intrinsic clearance, $CL_{int}$		clogP
	MLM	HLM	
AST	147	107	5.70
1	373.2	431.3	5.22
6	266	167.9	4.80
7	67.4	22.8	5.12
8	26.4	19.2	5.42
9	86.4	23	5.12
12	71.3	88.9	5.23
15	<11.6	<11.6	4.08
16	43.6	19.7	4.28
18	123.9	200.4	5.88
21	40.7	31.9	5.08
22	18.9	11.6	5.94
23	<11.6	<11.6	4.30
24	<11.6	<11.6	4.51
35	18.4	15.2	5.15

<sup>a</sup>MLM = mouse liver microsomes and HLM = human liver microsomes, expressed as percent (%) of drug remaining after incubation with microsomes for 30 min.  $CL_{int}$  = predicted intrinsic clearance in  $\mu\text{L}\cdot\text{min}^{-1}\cdot\text{mg}^{-1}$ . Mean from  $n \geq 2$  independent experiments. clogP = calculated lipophilicity of compounds, determined using StarDrop Software, version 6.11.

compound 1. Consistent with the literature, 3-/5- $\text{CH}_3$ -1,2,4-oxadiazole-containing analogues (i.e., 7 and 16) generally exhibited lower stability compared to 3-/5- $\text{CF}_3$ -1,2,4-oxadiazole-containing analogues (i.e., 8 and 24, Table 6).

**In Vitro Gametocytocidal and Liver-Stage Activity.** To assess activity of the analogues during other *Plasmodium* life-cycle stages in line with target candidate profile 3 (TCP3) for new antimalarials,<sup>25</sup> and based on previously observed multi-stage activity of AST and some of its analogues,<sup>11,26</sup> selected analogues from this series were assessed for their antiplasmodium sexual (gametocyte) and liver-stage properties.

Twenty analogues representing the structural diversity of each SAR were subjected to a dual-point screen against early- and late-stage gametocytes (EGs, II/III; LGs, IV/V) at 1.0 and 5.0  $\mu\text{M}$  (Supporting Information, Table S1) in a luciferase assay that allows for the determination of stage-specific gametocytocidal activity. None of the tested compounds showed high inhibitory activity (<50% inhibition) in both EGs and LGs at 1.0  $\mu\text{M}$ . However, nine analogues showed moderate (50–70% inhibition) to good activity (>70% inhibition) at 5  $\mu\text{M}$  and predominantly against EGs (Table S1).  $IC_{50}$  values were only determined for compounds showing activities >80% in the dual point assay. Notably, compounds devoid of the 4-CN-benzyl (or an aromatic moiety at benzimidazole *N*-1 position, i.e., AST) displayed higher activity against EGs than against LGs. Structurally related front-runners 23, 24, and 36 showed the highest activities with  $IC_{50}$ s in the low micromolar range ( $PfEG$   $IC_{50}$  = 1.18–1.67  $\mu\text{M}$ , Table 7) and >2-fold higher compared to AST's activity against LGs ( $PfLG$   $IC_{50}$  = 3.35  $\mu\text{M}$ , Supporting Information, Table S1).<sup>11</sup>

Activity against liver-stage infection was assessed using *P. berghei* in the HepG2 cell line. A preliminary single-point (1.0  $\mu\text{M}$ ) screen of only compounds with high *in vitro* ABS activity ( $PfNFS4$   $IC_{50}$  < 0.1  $\mu\text{M}$ ) and high microsomal metabolic stability (15, 23, 24, and 36) showed that only 23 and 24

**Table 7.** *In Vitro* Antiplasmodium Life Cycle Stage Activity Data

compound	$IC_{50}$ ( $\mu\text{M}$ )	
	$PfEG^a$	$PbHepG2^b$
AST		0.59 $\pm$ 0.21
23	1.52 $\pm$ 0.25	0.49 $\pm$ 0.18
24	1.67 $\pm$ 0.28	0.21 $\pm$ 0.09
36	1.18 $\pm$ 0.28	

<sup>a</sup>Early-stage gametocytes (EG stages I/III), reference drug: methylene blue ( $PfEG$   $IC_{50}$  = 0.2  $\mu\text{M}$ ). <sup>b</sup>*P. berghei* (*Pb*)-infected HepG2 cells, reference drug: primaquine ( $IC_{50}$  = 6.0  $\pm$  1.4  $\mu\text{M}$ ).

exhibited >75% reduction of parasite load with  $IC_{50}$ s of 0.49 and 0.21  $\mu\text{M}$ , respectively (Table 7 and Figure 3). HepG2 cell

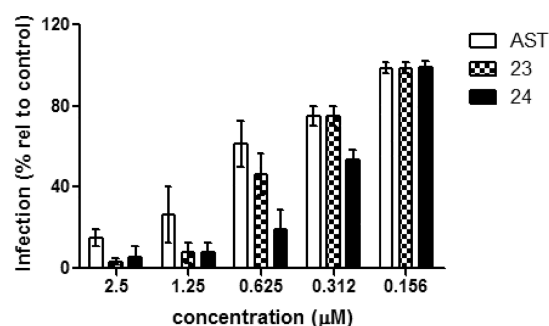


**Figure 3.** Concentration-dependent inhibition of *P. berghei*-sporozoite infection in HepG2 cells. Values are mean, and error bars are standard deviation normalized from untreated cells (negative control).

confluency was assessed in parallel for each compound, as a measure of cytotoxicity (Supporting Information, Table S2). Gratifyingly, no cytotoxicity was observed for all four compounds. (SIs > 80).

**In Vitro hERG Channel Inhibition Activity.** Representative analogues from the five SARs were profiled for the potential for cardiotoxicity risk by assessing their hERG  $K^+$  channel inhibitory activity (Table 8). The selection was made to best represent the various approaches used toward attenuating the hERG liability.

Although hERG inhibition is still an issue, all tested compounds showed lower hERG inhibitory concentrations ( $IC_{50}$  > 0.10  $\mu\text{M}$ ) compared to AST. Zwitterion furnishing compounds (42 and 69) and amides (44 and 50: hERG  $IC_{50}$   $\geq$  30  $\mu\text{M}$ ) displayed the least hERG channel inhibitory activity, albeit accompanied by poor selectivities (hERG SI < 18), as a result of equally low *in vitro* *Pf* activity. Similarly, removal of an aromatic moiety (i.e., 16), ring saturation (i.e., 18) and other lipophilicity-lowering strategies (i.e., 67) proved ineffective toward achieving high selectivity over hERG. Generally, high *Pf* inhibitors also produced relatively high hERG channel inhibition and vice versa. However, higher selectivities (hERG SI  $\geq$  19) were generally achieved in analogues with exceptional potency against *Pf*. These notably include 1,2,4-oxadiazole derivatives containing  $\text{CF}_3$  (23 and 10) and *t*-butyl (36) groups. Front-runner compound 23 (hERG  $IC_{50}$  = 0.63  $\mu\text{M}$ ; SI = 53) represents  $\sim$ 1071-fold higher selectivity compared to AST (hERG  $IC_{50}$  = 0.0042  $\mu\text{M}$ ).

**Cytotoxicity.** Analogues showing high antiplasmodium activity ( $PfNFS4$ - $IC_{50}$  < 0.10  $\mu\text{M}$ ) were profiled for cytotoxicity against the Chinese Hamster Ovary (CHO) cell

Table 8. Cytotoxicity (CHO) and hERG K<sup>+</sup> Channel Inhibitory Activity Results of Selected Analogues

No.	Structure	IC <sub>50</sub> (μM)		clogP	No.	Structure	IC <sub>50</sub> (μM)		clogP
		CHO <sup>a</sup> (SI) <sup>c</sup>	hERG <sup>b</sup> (SI) <sup>c</sup>				CHO <sup>a</sup> (SI) <sup>c</sup>	hERG <sup>b</sup> (SI) <sup>c</sup>	
AST		29.6 (344)	0.0042 (0.049)	5.70	21		5.63 (128)	0.25 (5.68)	5.08
1		12.4 (289)	-	5.22	22		3.33 (111)	-	5.94
6		16.6 (187)	-	4.80	23		1.96 (163)	0.63 (52.5)	4.30
7		5.87 (115)	-	5.12	24		3.18 (48.2)	0.86 (13)	4.51
8		3.85 (175)	-	5.42	29		-	0.13 (0.33)	5.02
9		19.7 (203)	0.10 (1.45)	5.12	36		4.69 (73.3)	1.35 (21.1)	5.15
10		0.75 (34)	0.47 (19)	5.42	42		-	>30 (~5.0)	3.34
12		38.9 (525)	-	5.23	44		-	>30 (≥17.3)	3.00
15		3.56 (64.7)	-	4.08	50		-	>30 (≥8.81)	2.25
16		9.08 (275)	0.35 (10.6)	4.28	67		-	0.49 (0.11)	3.53
18		44.4 (477)	0.89 (9.56)	5.88	69		-	28.7 (≤4.7)	3.73

<sup>a</sup>Chinese hamster ovary cell line (CHO). <sup>b</sup>Human ether-a-go-go related gene (hERG). <sup>c</sup>Selectivity index, SI = [(PfNF54 IC<sub>50</sub>)/(hERG IC<sub>50</sub>) or (PfNF54 IC<sub>50</sub>)/(CHO IC<sub>50</sub>)]; clogP = calculated lipophilicity, determined using StarDrop Software, version 6.11; MB = methylene blue.

line. No cytotoxicity was observed in this cell line as all the tested compounds displayed ideal selectivity margins (SI > 34, Table 8).

**In Vivo Efficacy in Mice.** Compounds 15, 23, and 24 (Table 9) were assessed for their *in vivo* efficacy in the *P. berghei* mouse infection model of malaria based on their high *in*

Table 9. *In Vivo* Efficacy after Oral Dosing in *P. Berghei*-Infected Mice at  $4 \times 50 \text{ mg}\cdot\text{kg}^{-1}$ 

Parameter	15	23	24
	dose ( $\text{mg}\cdot\text{kg}^{-1}$ )	$4 \times 50$	$4 \times 50$
activity (%)	40	99.5	90
MSD <sup>b</sup>	4 <sup>a</sup>	14	9

<sup>a</sup>Mice were euthanized on day 4 in order to prevent expected death otherwise occurring at day 6 due to high parasitemia. <sup>b</sup>MSD = mean survival days.

Table 10. Mouse Pharmacokinetic Parameters of 15 and 23

parameter	15			23		
	iv	oral		iv	oral	
dose ( $\text{mg}\cdot\text{kg}^{-1}$ )	3	10	50	3	10	50
$C_{\text{max}}$ ( $\mu\text{M}$ )		1	5.9		0.3	1.5
$T_{\text{max}}$ (h)		1.5	3.0		0.7	1.7
apparent $t_{1/2}$ (h)	11.6	10.3	9.2	4.2	1.1	10.2
$CL_{\text{int}}$ ( $\text{mL}\cdot\text{min}^{-1}\cdot\text{kg}^{-1}$ )	16.6			71.7		
$V_d$ ( $\text{L}\cdot\text{kg}^{-1}$ )	13.6			26.6		
$AUC_{0-\infty}$ ( $\mu\text{M}\cdot\text{min}^{-1}$ )	550	535	5548	93.4	48	1429
F (%)		29.3	61		15.6	93.3

*in vitro* activity (*Pf*NF54  $IC_{50} < 0.10 \mu\text{M}$ ), solubility, and metabolic stability (MLMs  $CL_{\text{int}} < 11.6 \mu\text{L}\cdot\text{min}^{-1}\cdot\text{mg}^{-1}$ ). In a standard quadrupole oral dose regimen of  $50 \text{ mg}\cdot\text{kg}^{-1}$ , 15, 23, and 24 showed 40, 99.5, and 90% reduction in parasitemia, respectively, relative to untreated mice (Table 9).

The high efficacy of 23 correlated to its high *in vitro* potency (*Pf*NF54  $IC_{50}$   $0.012 \mu\text{M}$ ), although curative effects were not observed at this dose (mouse mean survival of <30 days, Table 8). Chloroquine (CQ) was used as the reference drug, achieving 99.9% reduction in parasitemia when dosed orally at  $4 \times 30 \text{ mg}\cdot\text{kg}^{-1}$ , with a mouse mean survival of 24 days.

**Pharmacokinetic Studies in Mice.** When dosed intravenously (IV,  $3 \text{ mg}\cdot\text{kg}^{-1}$ ), 15 showed low clearance from blood ( $16.6 \text{ mL}\cdot\text{min}^{-1}\cdot\text{kg}^{-1}$ , Table 9) with moderate tissue distribution ( $13.6 \text{ L}\cdot\text{kg}^{-1}$ ) resulting in a long half-life (11.6 h). Oral dosing of 15 at  $10 \text{ mg}\cdot\text{kg}^{-1}$  revealed rapid absorption ( $T_{\text{max}} = 1.5 \text{ h}$ ) with moderate bioavailability (29.3%) (Table 10).

On the other hand, IV dosing of 23 at  $3 \text{ mg}\cdot\text{kg}^{-1}$  showed rapid clearance ( $71.7 \text{ mL}\cdot\text{min}^{-1}\cdot\text{kg}^{-1}$ ), albeit tissue distribution was high ( $26.6 \text{ L}\cdot\text{kg}^{-1}$ ) with a moderate half-life (4.2 h). Orally, 23 ( $T_{\text{max}} = 0.7 \text{ h}$ ) was absorbed 2-fold faster than 15 at  $10 \text{ mg}\cdot\text{kg}^{-1}$ , and bioavailability was equally 2-fold lower and suboptimal (15.6%) at that dose. However, 23 displays a dose-dependent PK profile, as demonstrated by a greater-than dose proportional increase in oral exposure at  $50 \text{ mg}\cdot\text{kg}^{-1}$  relative to the  $10 \text{ mg}\cdot\text{kg}^{-1}$  dose.

This increased *in vivo* exposure combined with the higher *in vitro* whole-cell *Pf* potency against ABS (23  $IC_{50} = 0.012 \mu\text{M}$

vs 15  $IC_{50} = 0.055 \mu\text{M}$ ) likely explains the better *in vivo* efficacy of 23.

**Mechanistic Studies. Live-Cell Microscopy Assay.** To shed light on the mechanism of action (MoA) of this class of compounds, 23 was initially investigated for its intrinsic fluorescence for *P. falciparum* live-cell imaging of using a fluorimeter. Excitation between 200 and 400 nm and emission between 400 and 800 nm at  $1.0 \mu\text{M}$  showed no significant response compared to the blank in both DCM and DMSO (Figure S3). This prompted the attachment of an extrinsic fluorophore to enable live-cell imaging. NBD was chosen based on its ready availability, small size, and stability over a biologically relevant pH range.<sup>27</sup> Its attachment point to 23 at N-1 was solely guided by SAR studies already described. Gratifyingly, the NBD-labeled derivative (probe) retained submicromolar *in vitro Pf* activity (23-NBD, *Pf*NF54  $IC_{50} = 0.140 \mu\text{M}$ ; Table 2). The probe was subjected to super-resolution structured illumination microscopy (SR-SIM) to assess subcellular accumulation in *Pf*-infected cells. This was carried out using commercially available organelle trackers LysoTracker Red, MitoTracker Deep Red, DRAQ5, ER-Tracker Red, and Nile Red (Figure 5A–E).

These fluorescent dyes are capable of illuminating respective membranes of acidic organelles like the parasite's digestive vacuole (DV), the mitochondrion, nucleus, endoplasmic reticulum, and lipids, respectively.<sup>28–30</sup>

The result revealed complete accumulation between 23-NBD and the LysoTracker Red (Figure 5A). Regions of highest accumulation were observed around the hemozoin (Hz) crystals, thereby implicating the parasite's digestive

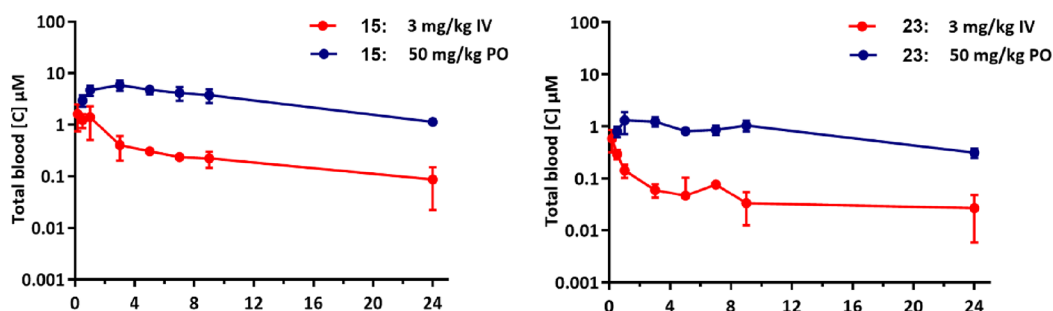


Figure 4. Blood concentrations of 15 and 23 following intravenous (iv) and oral (p.o.) dosing in healthy BalbC mice.

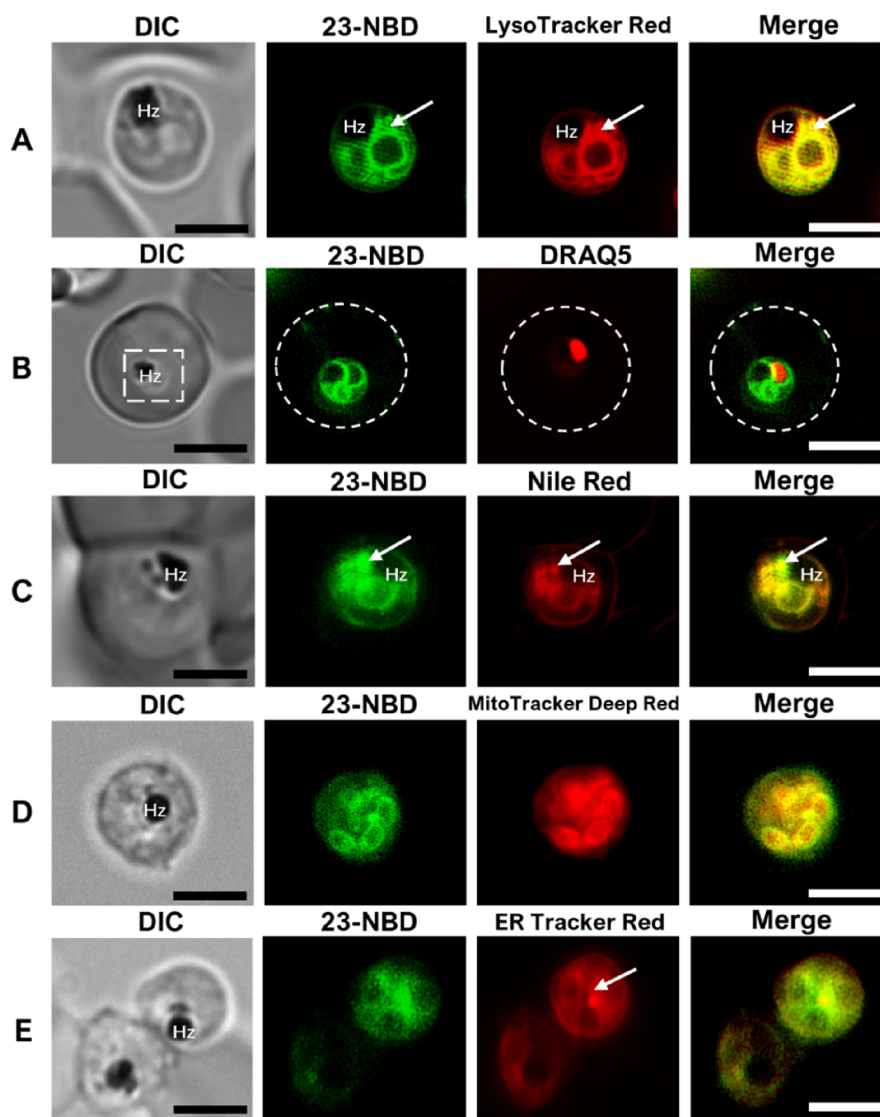
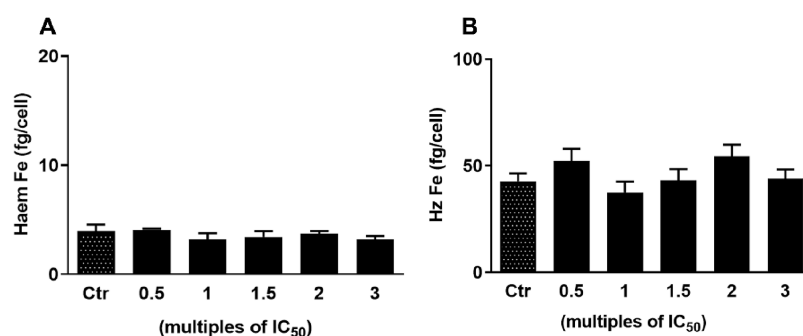


Figure 5. Live-cell SR-SIM of *P. falciparum*-infected erythrocyte treated with 23-NBD (green, panels A–E), with LysoTracker Red (red, panel A), with nuclear marker DRAQ5 (red, panel B), with lipid marker Nile Red (red, panel C), with MitoTracker Deep Red (red, panel D), and with ER Tracker Red (red, panel E). White arrows indicate areas of intense localization of the dye and regions of complete overlap are shown in the merged image (yellow). Scale bars: 5  $\mu\text{m}$ . Hz: Hemozoin; DIC: differential interference contrast.

vacuole as a plausible site of action of 23-NBD. Conversely, no colocalization was observed between 23-NBD and DRAQ5, eliminating the nucleus as a possible site of action (Figure 5B).

Lipids have been shown to play vital roles during the asexual blood stage of the parasite's life cycle. Precisely, neutral lipids have been implicated in the formation of  $\beta$ -hematin *in vitro* and

found at the site of Hz formation *in vivo*. It is believed that neutral lipids may serve as a site for Hz biocrystallization.<sup>31</sup> Following significant accumulation of 23-NBD around the Hz crystals, accumulation with the parasite's neutral lipids was also assessed. Neutral lipid droplets were found in close proximity to the Hz crystals, and these droplets colocalize with 23-NBD



**Figure 6.** Dose-dependent heme fractionation profiles of compound 23. The amount of “free” heme Fe (A) and hemozoin (Hz) Fe (B) at increasing concentrations of the compounds.

(Figure 5C). Coupled with accumulation of the NBD probe (23-NBD) in the DV, this data reiterates inhibition of hemozoin formation as a possible contributing mechanism of action for compound 23.

Aside from the digestive vacuole, the parasite possesses other organelles that equally play significant roles during the blood stage of the parasite’s life cycle such as the mitochondrion and the endoplasmic reticulum (ER). These organelles have previously been shown to be clinically relevant drug targets.<sup>32</sup> Consequently, we examined the ER and the mitochondrion in conjunction with 23-NBD. When incubated with MitoTracker Deep Red, we observed localized tube-like structures corresponding to the mitochondrion within the parasite. These structures partially colocalized with regions of high signal intensity from the 23-NBD (Figure 4D). This indicates some extent of colocalization between the mitochondrion and the compound. Also, significant colocalization was observed between the punctuate structure revealed by the ER Tracker Red and the diffused signal from the 23-NBD (Figure 5E), making both organelles a potential site of action of compound 23.

**Hemozoin Formation Inhibition.** To augment the results from the SIM-SR microscopy, which suggests inhibition of hemozoin formation as a plausible MoA of this class of compounds, and based on precedence from previous findings on AST and its analogues,<sup>7,11,12</sup> a selected number of active analogues across the SAR ( $PfNFS4-IC_{50} < 0.100 \mu M$ ) including 23 were evaluated for their inhibition of  $\beta$ -hematin ( $\beta H$ ) formation (Supporting Information, Table S4).<sup>33</sup> We conjured a  $100 \mu M$  discriminatory  $IC_{50}$  to identify strong inhibitors from this assay. Eight (8) of the 14 tested compounds blocked  $\beta H$  formation (Figure S3), while three (3) compounds (8, 10, and 21) displayed activities comparable to standard  $\beta H$  formation inhibitors such as amodiaquine ( $IC_{50}$ :  $10 \pm 2 \mu M$ ) and chloroquine ( $IC_{50}$ :  $22 \pm 2 \mu M$ ). A weak but positive correlation ( $r^2 = 0.1356$ ) was established between inhibition of  $\beta H$  formation and *in vitro* *Pf* activity (Supporting Information, Figure S3).

Furthermore, front-runner 23 was subjected to the cellular heme speciation assay to delineate its dose-dependent effect on various heme species in the parasite and assess its ability to inhibit intracellular Hz formation in *Pf* parasites. Despite its high activity in the pyridine-based  $\beta H$  assay (Table S3), 23 did not produce a statistically significant concentration-dependent increase in the levels of free heme relative to that of Hz (Figure 6 and Supporting Information, Table S3). This disconnect may in part be attributable to the limitations of *in vitro*  $\beta H$  assay in recapitulating the complex physiology involving intracellular

drug activity such as membrane permeation and accumulation in the digestive vacuole (DV).

## CONCLUSIONS

A novel set of 1,2,4-oxadiazole analogues of AST with high metabolic stability have been identified through metabolic stability-driven optimization of compound 1. Various approaches including bioisosterism and lipophilicity-reduction-driven modifications have been used, leading to the identification of 23, which demonstrates high *in vivo* efficacy in the *P. berghei* mouse infection model of malaria. Additionally, analogues showing high early-stage (EG, stage I/III) gametocytocidal activity, liver-stage activity, and absence of cytotoxicity against the CHO and HepG2 cell lines have been identified. The SAR from this work reaffirms the significance of the 4-amino piperidine moiety as an essential pharmacophoric component in AST analogues for antiplasmodium activity. This work has revealed that with a 3-CH<sub>3</sub>/3-CF<sub>3</sub>/3-*tert*-butyl-1,2,4-oxadiazole moiety at the 4-position of the lateral phenyl group, the benzyl moiety at benzimidazole *N*-1 is not required for asexual-blood stage (ABS) antiplasmodium activity. Removal of the benzyl moiety while retaining a 1,2,4-oxadiazole functionality in the lateral phenyl group produces high *Pf* activity, high *in vitro* metabolic stability, low lipophilicity, and low molecular weight, which benefit solubility and selectivity over hERG. Although several analogues still display  $\beta$ -hematin inhibition and significant amounts 23 accumulate in and around the parasite’s DV, 23 does not induce any statistically significant effect on the levels of heme or Hz in *Pf*. It is worth noting that inhibiting the formation of Hz is only one of many processes in the DV that can be inhibited by 23 to lead to the parasite’s death. We speculate that although inhibiting the formation of Hz might not be the primary MoA of 23, the compound could be affecting other processes in the DV. Also, there is the possibility of a novel target at play in the other organelles associated with 23. Compound 23 is the first direct analogue of AST to demonstrate multi-stage activity, high *in vivo* efficacy, with >1000-fold better hERG selectivity compared to AST, while retaining ideal drug-like properties. Further PK and hERG optimization into safer margins by utilizing other approaches not explored in this work as well as further studies into their MoA is warranted.

## EXPERIMENTAL SECTION

All commercially available chemicals were purchased from either Sigma-Aldrich (Germany) or Combi-Blocks (United States). <sup>1</sup>H NMR (all intermediates and final compounds) and <sup>13</sup>C NMR (for

target compounds only) spectra were recorded on a Bruker Spectrometry at 300, 400, or 600 megahertz (MHz). Melting points for all target compounds were determined using a Reichert-Jung Thermovar hot-stage microscope coupled to a Reichert-Jung Thermovar digital thermometer (20–350 °C range). Reaction monitoring using analytical thin-layer chromatography (TLC) was performed on aluminum-backed silica-gel 60 F<sub>254</sub> (70–230 mesh) plates with detection and visualization done using (a) UV lamp (254/366 nm), (b) iodine vapors, or (c) ninhydrin spray reagent. Column chromatography was performed with Merck silica-gel 60 (70–230 mesh). Chemical shifts ( $\delta$ ) are reported in ppm downfield from trimethylsilane (TMS) as the internal standard. Coupling constants ( $J$ ) were recorded in Hertz (Hz). Purity of compounds was determined by an Agilent 1260 Infinity binary pump, Agilent 1260 Infinity diode array detector, Agilent 1290 Infinity column compartment, Agilent 1260 Infinity standard autosampler, and Agilent 6120 quadrupole (single) mass spectrometer, equipped with APCI and ESI multi-mode ionization source. All compounds tested for biological activity were confirmed to have  $\geq 95\%$  purity by HPLC. Solubility, biological assays, and any experimental data not shown below (i.e., NMR of compound intermediates) are fully supplied and detailed in the Supporting Information.

**General Procedure 1: Synthesis of N-Hydroxyamidines (2a and 31a–e).** To a solution of nitrile (1 equiv) in absolute EtOH (0.10 M) was added NH<sub>2</sub>OH·HCl (1.2 equiv), followed by Et<sub>3</sub>N (1.2 equiv) and 8-hydroxyquinolone (10 mol %). The resulting mixture was refluxed at 79 °C for 1.5 h. After completion, the solvent was evaporated *in vacuo*, and the residue was dissolved with H<sub>2</sub>O (10 mL) and acidified to pH 3 using 10% HCl. The precipitate was filtered off and again washed with 10% HCl and dried.

**4-(2-Bromoethyl)-N-hydroxybenzimidamide (2a).** Obtained from 4-(2-bromoethyl)benzimidamide as a light green crystalline solid (0.57 g, 82%). <sup>1</sup>H NMR (300 MHz, DMSO-*d*<sub>6</sub>):  $\delta$  9.57 (s, 1H), 7.61 (d,  $J$  = 8.3 Hz, 2H), 7.27 (d,  $J$  = 8.3 Hz, 2H), 5.75 (s, 2H), 3.74 (t,  $J$  = 7.1 Hz, 2H), 3.14 (t,  $J$  = 7.1 Hz, 2H). LC–MS (APCI+/ESI): found  $m/z$  = 244.0, 245.0 [M + H]<sup>+</sup> (calcd. for C<sub>9</sub>H<sub>11</sub>BrN<sub>2</sub>O, 243.01, 244.01). HPLC purity: 98%,  $t_R$  = 0.318 min.

**N'-Hydroxyisobutyrimidamide (31a).** Obtained from isobutyronitrile (0.250 g, 3.61 mmol) as a pale-yellow solid (0.34 g, 92%). <sup>1</sup>H NMR (400 MHz, DMSO-*d*<sub>6</sub>):  $\delta$  8.90 (s, 1H), 6.51 (s, 2H), 2.55 (hept,  $J$  = 5.9 Hz, 1H), 1.05 (d,  $J$  = 5.9 Hz, 6H).

**3-(4-(2-Bromoethyl)phenyl)-1,2,4-oxadiazole (2b).** A solution of 2a (0.063 g, 0.26 mmol) in CH(EtO)<sub>3</sub> (1.5 mL) was charged with pyridine (1.5 mL) and catalytic amount of BF<sub>3</sub>·OEt<sub>2</sub> was stirred at 80 °C for 1 h. After the completion, the solvent was removed *in vacuo*, and the product was obtained by purification by flash column chromatography using 0–10% EtOAc/hexanes as a white crystalline solid (0.05 g, 51%). <sup>1</sup>H NMR (300 MHz, methanol-*d*<sub>4</sub>):  $\delta$  9.24 (s, 1H), 8.04 (d,  $J$  = 8.3 Hz, 2H), 7.43 (d,  $J$  = 8.3 Hz, 2H), 3.81 (t,  $J$  = 7.1 Hz, 2H), 3.13 (t,  $J$  = 7.0 Hz, 2H). LC (APCI+/ESI): HPLC purity: 98%,  $t_R$  = 0.318 min.

**3-(4-(2-Bromoethyl)phenyl)-5-methyl-1,2,4-oxadiazole (2c).** A mixture of 2a (0.10 g, 0.41 mmol) and acetyl chloride (350  $\mu$ L, 0.49 mmol) was refluxed in THF at 65 °C for 30 min. At completion, excess acetyl chloride and THF were evaporated under reduced pressure and the reaction mixture was quenched with H<sub>2</sub>O (5 mL). This mixture was extracted with DCM (3  $\times$  15 mL). Combined organic extracts were dried over anhydrous Na<sub>2</sub>SO<sub>4</sub> and evaporated off solvent under vacuum to afford product as a white crystalline solid (0.17 g, 80%). <sup>1</sup>H NMR (300 MHz, DMSO-*d*<sub>6</sub>):  $\delta$  7.68 (d,  $J$  = 8.3 Hz, 2H), 7.38 (d,  $J$  = 8.3 Hz, 2H), 3.76 (t,  $J$  = 7.0 Hz, 2H), 3.19 (t,  $J$  = 7.0 Hz, 2H), 2.17 (s, 3H). LC (APCI+/ESI): HPLC purity: 99%,  $t_R$  = 0.318 min.

**3-(4-(2-Bromoethyl)phenyl)-5-(trifluoromethyl)-1,2,4-oxadiazole (2d).** A mixture of 2a (0.10 g, 0.41 mmol) in 4 mL of pyridine and trifluoroacetic acid anhydride (172  $\mu$ L, 1.23 mmol) was stirred at room temperature (19 °C) for 20 min. The mixture was poured in ice H<sub>2</sub>O (10 mL) and extracted with ethyl acetate (3  $\times$  15 mL). The combined organic extracts were washed with brine and dried over anhydrous Na<sub>2</sub>SO<sub>4</sub>. The product was obtained after flash column

chromatography using 0–10% EtOAc/hexanes as pale-yellow oil (0.15 g, 76%). <sup>1</sup>H NMR (300 MHz, DMSO-*d*<sub>6</sub>):  $\delta$  8.16 (d,  $J$  = 8.2, 2H), 7.49 (d,  $J$  = 8.2, 2H), 3.80 (t,  $J$  = 7.0 Hz, 2H), 3.24 (t,  $J$  = 7.0 Hz, 2H). HPLC purity: 97%,  $t_R$  = 3.406 min.

**General Procedure 2: Synthesis of Intermediates 3a–3e.** To a solution of 4-(2-bromoethyl) benzoic acid (1 equiv) in DCM under ice, DMAP (0.1 equiv), EDCI (1.5 equiv), and Et<sub>3</sub>N (1.5 equiv) were added, and the solution was stirred at room temperature (21 °C) for 30 min. The appropriate amine (1.0 equiv) was then added dropwise, and the resulting solution was stirred at room temperature for 2 h. After completion, the reaction was diluted with another aliquot of initial amount of DCM and washed with saturated NaHCO<sub>3</sub> ( $\times$ 3) followed by H<sub>2</sub>O ( $\times$ 2) and then brine ( $\times$ 1). The DCM phase was then dried over anhydrous Na<sub>2</sub>SO<sub>4</sub>, the solvent was evaporated *in vacuo*, and products were obtained after washing with Et<sub>2</sub>O.

**(S)-4-(2-Bromoethyl)-N-(1-hydroxypropan-2-yl)benzamide (3a).** Obtained from (S)-2-aminopropan-1-ol (0.055 g, 0.73 mmol) as a white solid (0.168 g, 80%). <sup>1</sup>H NMR (300 MHz, methanol-*d*<sub>4</sub>):  $\delta$  7.89 (d,  $J$  = 8.2 Hz, 2H), 7.13 (d,  $J$  = 8.2 Hz, 2H), 3.71 (qt,  $J$  = 6.5, 6.2 Hz, 1H), 3.48 (t,  $J$  = 7.0 Hz, 2H), 3.12 (d,  $J$  = 6.2 Hz, 2H), 2.96 (t,  $J$  = 7.0 Hz, 2H), 1.65 (d,  $J$  = 6.5 Hz, 3H). LC–MS (APCI+/ESI): found  $m/z$  = 286.0, 288.0 [M + H]<sup>+</sup> (calcd. for C<sub>12</sub>H<sub>16</sub>BrNO<sub>2</sub>, 285.04, 287.03). HPLC purity: 96%,  $t_R$  = 2.593 min.

**Methyl 4-(2-bromoethyl) Benzoate (3f).** To a solution of 4-(2-bromoethyl) benzoic acid (5 g, 21.8 mmol) in 4:1 toluene/methanol (60 mL) under ice was added dropwise a solution of 2 M of TMS-CHN<sub>2</sub> in hexanes until the yellow color no longer dissipated (about 28 mL added in 25 min). The mixture was evaporated *in vacuo* to dryness followed by purification *via* flash column chromatography using 0–20% EtOAc/hexanes as the eluent. The product was obtained as colorless/clear oil (5.15 g, 97%). <sup>1</sup>H NMR (400 MHz, DMSO-*d*<sub>6</sub>):  $\delta$  7.96 (d,  $J$  = 8.4 Hz, 2H), 7.20 (d,  $J$  = 8.4 Hz, 2H), 3.85 (s, 3H), 3.54 (t,  $J$  = 4.4 Hz, 2H), 3.14 (t,  $J$  = 4.4 Hz, 2H). HPLC purity: 99%,  $t_R$  = 2.955 min.

**General Procedure 3: Synthesis of Intermediates 4a–4c.** To a stirring suspension of amide 3a–3c (1 equiv) in DCM (5 mL) was added Et<sub>3</sub>N (2 equiv) followed by tosyl chloride (2 equiv). The mixture was stirred at 30 °C for 30 min. DCM was removed under vacuum followed by addition of EtOAc (15 mL). The mixture was washed with NaHCO<sub>3</sub> (2  $\times$  10 mL) and brine (10 mL) and then dried over anhydrous Na<sub>2</sub>SO<sub>4</sub> and evaporated off the solvent under vacuum. Crude solid products were purified by column chromatography using 0–25% EtOAc/hexane gradient as an eluent.

**(S)-2-(4-(2-Bromoethyl)phenyl)-4-methyl-4,5-dihydrooxazole (4a).** Obtained from 3a (0.10 g, 0.35 mmol) as a white solid (0.066 g, 70%). <sup>1</sup>H NMR (300 MHz, methanol-*d*<sub>4</sub>):  $\delta$  8.01 (d,  $J$  = 8.2 Hz, 2H), 7.41 (d,  $J$  = 8.2 Hz, 2H), 4.11 (dd,  $J$  = 10.1, 7.9 Hz, 1H), 3.96 (dd,  $J$  = 7.9, 6.2 Hz, 1H), 3.67 (t,  $J$  = 7.1 Hz, 2H), 3.33 (ddq,  $J$  = 10.1, 6.2, 6.0 Hz, 1H), 3.24 (t,  $J$  = 7.1 Hz, 2H), 1.95 (d,  $J$  = 6.0 Hz, 3H). LC–MS (APCI+/ESI): found  $m/z$  = 268.0, 270.0 [M + H]<sup>+</sup> (calcd. for C<sub>12</sub>H<sub>14</sub>BrNO, 267.03, 267.02). HPLC purity: 98%,  $t_R$  = 2.745 min.

**1-Isopropyl-N-(piperidin-4-yl)-1H-benzo[d]imidazol-2-amine (14c).**<sup>12</sup> White solid (0.336 g, 86%). R<sub>f</sub> (10% MeOH/DCM), 0.23. <sup>1</sup>H NMR (400 MHz, methanol-*d*<sub>4</sub>):  $\delta$  7.37 (dd,  $J$  = 7.7, 1.2 Hz, 1H), 7.30 (dd,  $J$  = 8.0, 1.2 Hz, 1H), 6.96 (ddd,  $J$  = 8.0, 7.2, 1.3 Hz, 1H), 6.77 (ddd,  $J$  = 7.7, 7.2, 1.3 Hz, 1H), 4.55 (hept,  $J$  = 6.8 Hz, 1H), 4.20 (t,  $J$  = 10.8, 4.0 Hz, 1H), 3.98–3.91 (m, 2H), 3.05–2.96 (m, 2H), 2.11–2.03 (m, 2H), 1.59 (d,  $J$  = 6.8 Hz, 6H), 1.55–1.47 (m, 2H). LC–MS (APCI+/ESI): found  $m/z$  = 259.2 [M + H]<sup>+</sup> (calcd. for C<sub>15</sub>H<sub>22</sub>N<sub>4</sub>, 258.18). Purity: 99%,  $t_R$  = 0.877 min.

**General Procedure 4: N-Alkylation of Benzimidazole.** A mixture of 2-chlorobenzimidazole (1 equiv), alkyl halide (1.2 equiv), and K<sub>2</sub>CO<sub>3</sub> (1.2 equiv) was stirred at room temperature (22 °C) in acetone for 2 h. After completion, the solvent was removed *in vacuo*. H<sub>2</sub>O was added to the residue followed by extracting with DCM ( $\times$ 3). Combined organic layers were washed with brine and dried over anhydrous Na<sub>2</sub>SO<sub>4</sub>, and the solvent was evaporated *in vacuo* to give the crude residue, which was triturated with *n*-pentane to afford the product.

4-((2-Chloro-1-benzo[d]imidazol-1-yl)methyl)benzotrile (25). Obtained from 2-chlorobenzimidazole (3.50 g, 22.9 mmol) and 4-(bromomethyl)benzotrile (5.4 g, 27.6 mmol) as a white crystalline solid (6.00 g, 98%).  $R_f$  (5% MeOH/DCM) 0.65.  $^1\text{H NMR}$  (400 MHz, methanol- $d_4$ ):  $\delta$  7.68 (d,  $J$  = 8.4 Hz, 2H), 7.63 (dd,  $J$  = 6.0, 0.8 Hz, 1H), 7.39 (dd,  $J$  = 6.5, 1.0 Hz, 1H), 7.34 (d,  $J$  = 8.4 Hz, 2H), 7.31–7.27 (m, 2H), 5.59 (s, 2H). LC–MS (APCI<sup>+</sup>/ESI): found  $m/z$  = 267.9, 269.9  $[\text{M} + \text{H}]^+$  (calcd. for  $\text{C}_{15}\text{H}_{10}\text{ClN}_3$ , 267.06, 269.05). Purity: 99%,  $t_R$  = 2.505 min.

**General Procedure 5: Synthesis of 26a–c.** A mixture of 25 (1.0 equiv), an appropriate mono-*N*-Boc-protected cyclic diamine (1.5 equiv), and  $\text{Et}_3\text{N}$  (2.0 equiv) in toluene was irradiated in a microwave reactor at 150 °C for 5–30 min. The residue was cooled and diluted with 10% MeOH/DCM. The mixture was washed with saturated  $\text{NaHCO}_3$  solution (3 × 20 mL), and combined organic layers were washed with brine (10 mL) and further dried over anhydrous  $\text{Na}_2\text{SO}_4$ . The solvent was evaporated *in vacuo* to obtain a crude residue, which was either triturated with *n*-pentane (or  $\text{Et}_2\text{O}$ ) or purified *via* flash column chromatography (3–4% MeOH/DCM) to afford the pure products.

*tert*-Butyl (S)-3-((1-(4-Cyanobenzyl)-1H-benzo[d]imidazol-2-yl)amino)pyrrolidine-1-carboxylate (26a). Obtained from 25 (0.300 g, 1.12 mmol) and *tert*-butyl (S)-3-aminopyrrolidine-1-carboxylate (293  $\mu\text{L}$ , 1.68 mmol) as a light brown solid (0.304 g, 65%).  $R_f$  (10% MeOH/DCM), 0.50.  $^1\text{H NMR}$  (600 MHz, methanol- $d_4$ ):  $\delta$  7.70 (d,  $J$  = 8.3 Hz, 2H), 7.49 (dd,  $J$  = 7.9, 1.2 Hz, 1H), 7.38 (d,  $J$  = 8.3 Hz, 2H), 7.32 (ddd,  $J$  = 7.9, 7.0, 1.4 Hz, 1H), 7.28 (dd,  $J$  = 8.1, 1.2 Hz, 1H), 7.25 (ddd,  $J$  = 8.1, 7.0, 1.4 Hz, 1H), 5.62 (s, 2H), 4.70 (tt,  $J$  = 6.8, 4.2 Hz, 1H), 3.73 (dd,  $J$  = 12.9, 6.8 Hz, 1H), 3.55–3.47 (m, 2H), 3.40 (ddd,  $J$  = 11.5, 8.4, 5.7 Hz, 1H), 2.55 (ddd,  $J$  = 15.0, 8.4, 6.8 Hz, 1H), 2.29 (ddd,  $J$  = 11.5, 8.2, 4.1 Hz, 1H), 1.48 (s, 9H). LC–MS (APCI<sup>+</sup>/ESI): found  $m/z$  = 418.2  $[\text{M} + \text{H}]^+$  (calcd. for  $\text{C}_{24}\text{H}_{27}\text{N}_5\text{O}_2$ , 417.22). Purity: 99%,  $t_R$  = 2.801 min.

**General Procedure 6: N-Boc Deprotection (Synthesis of Compounds 14a–d, 27a–c, and 60a–k).** Respective *N*-Boc-protected amines were stirred in DCM and TFA (10 equiv) at 23 °C for 2 h. Following completion, DCM and TFA were evaporated *in vacuo*, and the residue was taken up in 50% MeOH/DCM. This solution was stirred with Amberlyst A-21 free base resin at room temperature (23 °C) until pH was neutral. The mixture was then filtered, and the filtrate was evaporated *in vacuo* to afford free amines.

(*R*)-4-((2-(Pyrrolidine-3-ylamino)-1H-benzo[d]imidazol-1-yl)methyl) Benzotrile (27a). Following general procedure 6, obtained from 26a (0.280 g, 0.67 mmol) as a pale-yellow solid (0.181 g, 85%).  $R_f$  (10% MeOH/DCM), 0.10.  $^1\text{H NMR}$  (600 MHz, methanol- $d_4$ ):  $\delta$  7.73 (d,  $J$  = 8.4 Hz, 2H), 7.55 (dd,  $J$  = 8.0, 1.2 Hz, 1H), 7.43 (d,  $J$  = 8.4 Hz, 2H), 7.38 (ddd,  $J$  = 8.0, 7.1, 1.5 Hz, 1H), 7.31 (dd,  $J$  = 8.2, 1.2 Hz, 1H), 7.29 (ddd,  $J$  = 8.2, 7.1, 1.4 Hz, 1H), 5.60 (s, 2H), 4.69 (tt,  $J$  = 6.7, 4.3 Hz, 1H), 3.79 (dd,  $J$  = 12.8, 6.7 Hz, 1H), 3.61–3.55 (m, 2H), 3.52 (ddd,  $J$  = 11.5, 8.2, 5.7 Hz, 1H), 2.56 (ddd,  $J$  = 14.7, 8.2, 6.7 Hz, 1H), 2.31 (ddd,  $J$  = 11.5, 8.2, 4.3 Hz, 1H). LC–MS (APCI<sup>+</sup>/ESI): found  $m/z$  = 318.2  $[\text{M} + \text{H}]^+$  (calcd. for  $\text{C}_{19}\text{H}_{19}\text{N}_5$ , 317.16). Purity: 99%,  $t_R$  = 2.499 min.

5,6-Difluoro-1-methyl-*N*-(piperidin-4-yl)-1H-benzo[d]imidazol-2-amine (60a). Following general procedure 6, obtained from 59a (0.160 g, 0.44 mmol) as a light brown solid (0.108 g, 93%).  $R_f$  (5% MeOH/DCM), 0.13.  $^1\text{H NMR}$  (400 MHz, methanol- $d_4$ ):  $\delta$  7.45 (dd,  $J$  = 7.4, 5.3 Hz, 1H), 7.34 (dd,  $J$  = 7.5, 5.5 Hz, 1H), 3.92 (tt,  $J$  = 11.2, 4.0 Hz, 1H), 3.52 (s, 3H), 3.19–3.10 (m, 2H), 3.05–2.96 (m, 2H), 2.10–1.98 (m, 2H), 1.49–1.38 (m, 2H). LC–MS (APCI<sup>+</sup>/ESI): found  $m/z$  = 267.1  $[\text{M} + \text{H}]^+$  (calcd. for  $\text{C}_{13}\text{H}_{16}\text{F}_2\text{N}_4$ , 266.13). Purity: 96%,  $t_R$  = 0.822 min.

1-Methyl-2-(piperidin-4-ylamino)-1H-benzo[d]imidazole-5-carbonitrile (60d). Following general procedure 7, obtained from 59d (0.500 g, 1.41 mmol) as an off-white solid (0.319 g, 89%).  $R_f$  (5% MeOH/DCM), 0.13.  $^1\text{H NMR}$  (400 MHz, methanol- $d_4$ ):  $\delta$  7.97 (d,  $J$  = 1.4 Hz, 1H), 7.78 (d,  $J$  = 7.5 Hz, 1H), 7.52 (dd,  $J$  = 7.5, 1.4 Hz, 1H), 3.94 (tt,  $J$  = 10.8, 4.0 Hz, 1H), 3.50 (s, 3H), 3.21–3.13 (m, 2H), 3.08–2.99 (m, 2H), 2.09–1.98 (m, 2H), 1.52–1.39 (m, 2H). LC–

MS (APCI<sup>+</sup>/ESI): found  $m/z$  = 256.2  $[\text{M} + \text{H}]^+$  (calcd. for  $\text{C}_{14}\text{H}_{17}\text{N}_5$ , 255.15). Purity: 99%,  $t_R$  = 0.699 min.

1-(2-Aminoethyl)-*N*-(piperidin-4-yl)-1H-benzo[d]imidazol-2-amine (60k). Following general procedure 6, obtained from 59k (0.490 g, 10.7 mmol) as a white solid (0.235 g, 85%).  $R_f$  (10% MeOH/DCM), 0.09.  $^1\text{H NMR}$  (300 MHz, DMSO- $d_6$ ):  $\delta$  8.45 (br-s, 3H), 7.30 (dd,  $J$  = 7.1, 1.7 Hz, 1H), 7.26 (dd,  $J$  = 7.1, 1.6 Hz, 1H), 7.07–6.92 (m, 2H), 4.28 (t,  $J$  = 6.6 Hz, 2H), 4.00 (tt,  $J$  = 10.3, 3.8 Hz, 1H), 3.42–3.29 (m, 2H), 3.22–2.90 (m, 4H), 2.24–2.03 (m, 2H), 1.78 (dtd,  $J$  = 14.2, 10.9, 3.9 Hz, 2H). LC–MS (APCI<sup>+</sup>/ESI): found  $m/z$  = 260.2  $[\text{M} + \text{H}]^+$  (calcd. for  $\text{C}_{14}\text{H}_{21}\text{N}_5$ , 259.18). Purity: 98%,  $t_R$  = 0.186 min.

*tert*-Butyl 4-Isothiocyantopiperidine-1-carboxylate (52). To a solution of *tert*-butyl 4-aminopiperidine-1-carboxylate (8.00 g, 39.9 mmol) in DMF (50 mL) at 0 °C was added 1,1'-thiocarbonyldiimidazole (7.82 g, 43.9 mmol). The reaction mixture was allowed to rise to room temperature (24 °C) and stirred for 20 h at that temperature. The solvent was taken off *in vacuo*, and the residue was dissolved in EtOAc and washed with  $\text{H}_2\text{O}$  (3 × 50 mL). The solvent was removed *in vacuo*, and the residue was triturated with hexane and filtered. The filtrate was treated with activated charcoal and filtered through Celite. Removal of the solvent afforded the product as colorless oil (7.52 g, 78%).  $^1\text{H NMR}$  (400 MHz, DMSO- $d_6$ ):  $\delta$  4.11–3.98 (m, 2H), 3.69 (tt,  $J$  = 11.3, 4.1 Hz, 1H), 3.09–2.94 (m, 2H), 2.17–2.05 (m, 2H), 1.92–1.83 (m, 2H), 1.45 (s, 9H).

**General Procedure 7: Synthesis of 2-Chlorobenzimidazoles 54a–c.** A mixture of commercially obtained benzene-1,2-diamines (1 equiv), 1,1'-carbonyldiimidazole (1.5 equiv), and DMAP (1.0 mol %) was dissolved in dry THF (10 mL), and the resulting mixture was stirred at 22 °C for 2–12 h. After completion, the solvent was evaporated *in vacuo* and  $\text{H}_2\text{O}$  (30 mL) was added to the resulting residue. Benzimidazol-2-one products were obtained quantitatively after filtering and subsequent oven drying. Crude benzimidazole-2-ones (1 equiv) were then treated with  $\text{POCl}_3$  (5.0 equiv) in a sealed tube and stirred at 110 °C for 12 h. The reaction mixture was then cooled to room temperature (22 °C), and excess  $\text{POCl}_3$  was evaporated under reduced pressure. The residue was taken up in EtOAc (20 mL) and neutralized using 15% NaOH under ice while stirring. After separation, the aqueous phase was further extracted with EtOAc (3 × 20 mL). The combined organic extracts were washed with brine solution (10 mL) and dried over anhydrous  $\text{Na}_2\text{SO}_4$ , and the solvent was evaporated *in vacuo*. Pure products were obtained after flash chromatography using 20–50% EtOAc/hexanes as an eluent.

2-Chloro-5,6-difluoro-1H-benzo[d]imidazole (54a). Obtained from 4,5-difluorobenzene-1,2-diamine (0.250 g, 1.73 mmol) as a reddish solid (0.278 g, 84%).  $R_f$  (5% MeOH/DCM), 0.76.  $^1\text{H NMR}$  (300 MHz, methanol- $d_4$ ):  $\delta$  7.54 (m, 2H). LC–MS (APCI<sup>+</sup>/ESI): found  $m/z$  = 189.0, 191.0  $[\text{M} + \text{H}]^+$  (calcd. for  $\text{C}_7\text{H}_3\text{ClF}_2\text{N}_2$ , 188.00, 189.99). Purity: 98%,  $t_R$  = 2.632 min.

**General Procedure 8: Synthesis of 55a–c.** A mixture of 54a–c (1 equiv), methyl iodide (1.2 equiv), and  $\text{K}_2\text{CO}_3$  (1.2 equiv) was stirred at room temperature (22 °C) in acetone for 2 h. After completion (monitored *via* TLC), the solvent was removed *in vacuo*.  $\text{H}_2\text{O}$  was added to the residue followed by extracting with DCM (×3). Combined organic layers were washed with brine and dried over anhydrous  $\text{Na}_2\text{SO}_4$ , and the solvent was evaporated *in vacuo* to give the crude residue, which was triturated with *n*-pentane to afford the product.

2-Chloro-5,6-difluoro-1-methyl-1H-benzo[d]imidazole (55a). Following the general procedure 2, obtained from 54a (0.250 g, 1.32 mmol) and methyl iodide (99  $\mu\text{L}$ , 1.58 mmol) as a light green solid (0.212 g, 79%).  $R_f$  (5% MeOH/DCM), 0.93.  $^1\text{H NMR}$  (400 MHz, methanol- $d_4$ ):  $\delta$  7.42 (dd,  $J$  = 7.4, 5.3 Hz, 1H), 7.27 (dd,  $J$  = 7.5, 5.5 Hz, 1H), 3.83 (s, 3H). LC–MS (APCI<sup>+</sup>/ESI): found  $m/z$  = 203.0, 205.0  $[\text{M} + \text{H}]^+$  (calcd. for  $\text{C}_8\text{H}_5\text{ClF}_2\text{N}_2$ , 202.01, 204.01). Purity: 99%,  $t_R$  = 2.587 min.

**General Procedure 9: Synthesis of 59a–c.** A mixture of 55a–c (1.0 equiv), *N*-Boc-4-amino piperidine (1.5 equiv), and  $\text{Et}_3\text{N}$  (2.0 equiv) was stirred at 155 °C in a sealed tube for 6–36 h. After

completion, the residue was cooled and diluted with 10% MeOH/DCM. The mixture was washed with saturated NaHCO<sub>3</sub> solution (×3) and then brine and dried over anhydrous Na<sub>2</sub>SO<sub>4</sub>. The solvent was evaporated *in vacuo* to obtain a crude residue, which was either triturated with *n*-pentane (or diethyl ether) or purified *via* flash column chromatography to afford the pure products.

**Ethyl 4-((5,6-Difluoro-1-methyl-1H-benzo[d]imidazol-2-yl)amino)piperidine-1-Carboxylate (59a).** Obtained from 55a (0.180 g, 0.88 mmol) and *tert*-butyl 4-aminopiperidine-1-carboxylate (0.265 g, 1.32 mmol) as a brown solid (0.184 g, 57%). *R<sub>f</sub>* (5% MeOH/DCM), 0.78. <sup>1</sup>H NMR (400 MHz, DMSO-*d*<sub>6</sub>): δ 7.40 (dd, *J* = 7.4, 5.3 Hz, 1H), 7.32 (dd, *J* = 7.5, 5.5 Hz, 1H), 6.69 (d, *J* = 7.6 Hz, 1H), 4.51–4.42 (m, 2H), 3.91 (tt, *J* = 11.2, 4.0 Hz, 1H), 3.52 (s, 3H), 3.09–2.98 (m, 2H), 2.15–2.06 (m, 2H), 1.59–1.51 (m, 2H), 1.39 (s, 9H). LC–MS (APCI<sup>+</sup>/ESI): found *m/z* = 367.2 [*M* + *H*]<sup>+</sup> (calcd. for C<sub>18</sub>H<sub>24</sub>F<sub>2</sub>N<sub>4</sub>O<sub>2</sub>, 366.19). Purity: 98%, *t<sub>R</sub>* = 2.579 min.

**General Procedure 10: Synthesis of 58a–h.** An *o*-halo-nitrobenzene (1.0 equiv), an appropriate amine (1.2 equiv), and K<sub>2</sub>CO<sub>3</sub> (1.5 equiv) were mixed in MeCN (10–15 mL). Et<sub>3</sub>N (1.5 equiv) was added, and the resulting mixture was stirred at 65 °C for 4–18 h. After completion, the mixture was cooled to room temperature (18 °C) followed by the addition of H<sub>2</sub>O (15 mL) and EtOAc (30 mL). The mixture was separated, and the aqueous phase was further extracted with EtOAc (2 × 15 mL). Combined organic phases were dried over anhydrous Na<sub>2</sub>SO<sub>4</sub>, and the solvent was evaporated *in vacuo*. Pure *o*-amino-nitrobenzene intermediates were obtained following recrystallization from ethanol and used in the next step.

To a solution of the crude *o*-amino-nitrobenzenes (1.0 equiv) in 1:1 MeOH/EtOAc (10–25 mL) was added 10% Pd/C (0.1 equiv), and the reaction mixture was stirred at 21 °C under a hydrogen (H<sub>2</sub>) atmosphere using a double-padded balloon for 12–36 h. After completion, the reaction mixture was filtered through a bed of Celite, and the filtrate was concentrated *in vacuo* to afford products. If required, flash column chromatography using 20–70% EtOAc/Hexanes was performed.

**3-Amino-4-(methylamino)benzonitrile (58a).** Obtained from 4-chloro-3-nitrobenzonitrile (0.500 g, 2.74 mmol) and methylamine (2 M solution in THF, 1.64 mL, 3.29 mmol) as a dark brown solid (0.319 g, 79% over two steps). *R<sub>f</sub>* (40% EtOAc/Hexane) 0.32. <sup>1</sup>H NMR (300 MHz, DMSO-*d*<sub>6</sub>): δ 7.58 (d, *J* = 1.6 Hz, 1H), 7.28 (dd, *J* = 8.0, 1.6 Hz, 1H), 6.21 (d, *J* = 8.0 Hz, 1H), 5.02 (s, 2H), 2.71 (s, 3H). Purity: 99%, *t<sub>R</sub>* = 0.153 min.

***tert*-Butyl (2-((2-Aminophenyl)amino)ethyl)carbamate (58h).** Obtained from 1-fluoro-2-nitrobenzene (1.60 g, 5.70 mmol) and *tert*-butyl (2-aminoethyl)carbamate (1.10 g, 6.84 mmol) as a dark brown solid (1.40 g, 98% over two steps). *R<sub>f</sub>* (40% EtOAc/Hexane), 0.21. <sup>1</sup>H NMR (300 MHz, DMSO-*d*<sub>6</sub>): δ 6.88 (t, *J* = 5.7 Hz, 1H), 6.55 (dd, *J* = 7.3, 1.6 Hz, 1H), 6.52–6.37 (m, 3H), 4.39 (br-s, 3H), 3.21–3.11 (m, 2H), 3.11–3.00 (m, 2H), 1.40 (s, 9H). LC–MS (APCI<sup>+</sup>/ESI): found *m/z* = 252.1 [*M* + *H*]<sup>+</sup> (calcd. for C<sub>13</sub>H<sub>21</sub>N<sub>3</sub>O<sub>2</sub>, 251.16). Purity: 98%, *t<sub>R</sub>* = 0.189 min.

**General Procedure 11: Synthesis of 59d–k.** To a solution of 58a–h (1 equiv) in MeCN (15 mL), isothiocyanate 52 (1.1 equiv) and Et<sub>3</sub>N (1.2 equiv) were added, and the mixture was refluxed at 85 °C for 1 h. DCC (1.2 equiv) was then added, and the reaction mixture was further refluxed at 85 °C for 11 h. After completion, MeCN was evaporated *in vacuo*, and the residue was adsorbed on silica gel. Pure products were obtained after purification *via* flash chromatography using 10% MeOH/DCM as an eluent.

***tert*-Butyl 4-((5-Cyano-1-methyl-1H-benzo[d]imidazol-2-yl)amino)piperidine-1-carboxylate (59d).** Obtained from 58a (0.280 g, 1.90 mmol) and 52 (0.507 g, 2.10 mmol) as a light brown solid (0.573 g, 85%). *R<sub>f</sub>* (5% MeOH/DCM), 0.53. <sup>1</sup>H NMR (400 MHz, DMSO-*d*<sub>6</sub>): δ 7.97 (d, *J* = 1.4 Hz, 1H), 7.78 (d, *J* = 7.5 Hz, 1H), 7.52 (dd, *J* = 7.5, 1.4 Hz, 1H), 6.75 (d, *J* = 7.5 Hz, 1H), 4.49–4.41 (m, 2H), 3.94 (tt, *J* = 10.8, 4.0 Hz, 1H), 3.50 (s, 3H), 3.08–2.95 (m, 2H), 2.10–2.01 (m, 2H), 1.50–1.43 (m, 2H), 1.43 (s, 9H). LC–MS (APCI<sup>+</sup>/ESI): found *m/z* = 356.2 [*M* + *H*]<sup>+</sup> (calcd. for C<sub>19</sub>H<sub>25</sub>N<sub>5</sub>O<sub>2</sub>, 355.20). Purity: 99%, *t<sub>R</sub>* = 2.397 min.

***tert*-Butyl 4-((1-(2-((*tert*-Butoxycarbonyl)amino)ethyl)-1H-benzo[d]imidazol-2-yl)amino)piperidine-1-carboxylate (59k).** Obtained from 58h (0.500 g, 2.00 mmol) and 52 (0.531 g, 2.18 mmol) as a white solid (0.780 g, 85%). *R<sub>f</sub>* (7% MeOH/DCM), 0.38. <sup>1</sup>H NMR (300 MHz, DMSO-*d*<sub>6</sub>): δ 7.19 (dd, *J* = 7.9, 1.2 Hz, 1H), 7.12 (dd, *J* = 8.0, 1.3 Hz, 1H), 7.00–6.78 (m, 3H), 6.25 (d, *J* = 7.6 Hz, 1H), 4.08–3.99 (m, 2H), 3.99–3.87 (m, 3H), 3.26–3.12 (m, 2H), 2.98–2.83 (m, 2H), 2.03–1.90 (m, 2H), 1.50–1.37 (m, 11H), 1.33 (s, 9H). LC–MS (APCI<sup>+</sup>/ESI): found *m/z* = 460.3 [*M* + *H*]<sup>+</sup> (calcd. for C<sub>24</sub>H<sub>37</sub>N<sub>5</sub>O<sub>4</sub>, 459.28). Purity: 98%, *t<sub>R</sub>* = 2.439 min.

**General Procedure 12: Synthesis of 6–13, 15–17, 23, 24, 28–30, 32, 61–68, and 70–72.** A solution of appropriate amine (1.0 equiv) and K<sub>2</sub>CO<sub>3</sub> (1.5 equiv) in MeCN was stirred under reflux at 80 °C for 30 min. An appropriate alkyl bromide (1.2 equiv) was added, and the mixture was further stirred under reflux at 85 °C for 5–24 h. After completion, MeCN was taken off under reduced pressure, and the residue was taken up in 10% MeOH/DCM and filtered. The filtrate was adsorbed on silica gel, after which column chromatography was performed using a 3–10% MeOH/DCM gradient as an eluent to afford the final compounds.

**4-((2-((1-(4-(1,2,4-Oxadiazol-3-yl)phenethyl)piperidin-4-yl)amino)-1-benzo[d]imidazol-1-yl)methyl) Benzonitrile (6).** Obtained from 5 (0.080 g, 0.24 mmol) and 2b (0.073 g, 0.29 mmol) as a pale-yellow solid (0.087 g, 72%); m.p.: 98–100 °C; *R<sub>f</sub>* (10% MeOH/DCM), 0.59. <sup>1</sup>H NMR (600 MHz, methanol-*d*<sub>4</sub>): δ 7.65 (d, *J* = 8.7 Hz, 2H), 7.63 (dd, *J* = 8.0 Hz, 2H), 7.42 (d, *J* = 8.7 Hz, 2H), 7.33 (dd, *J* = 7.9, 1.1 Hz, 1H), 7.24 (d, *J* = 8.0 Hz, 2H), 7.06 (ddd, *J* = 7.9, 7.2, 1.0 Hz, 1H), 7.00 (dd, *J* = 8.0, 1.0 Hz, 1H), 6.95 (ddd, *J* = 8.0, 7.2, 1.1 Hz, 1H), 5.37 (s, 2H, H<sup>5</sup>), 3.84 (tt, *J* = 11.1, 4.2 Hz, 1H), 3.06–3.01 (m, 2H), 2.94–2.87 (m, 2H), 2.70–2.66 (m, 2H), 2.36–2.30 (m, 2H), 2.12–2.08 (m, 2H), 1.67–1.58 (m, 2H). <sup>13</sup>C NMR (151 MHz, methanol-*d*<sub>4</sub>): δ 154.10, 145.93, 142.30, 141.53, 140.68, 133.85, 132.25 (2C), 131.97 (2C), 129.47 (2C), 127.13 (2C), 121.34, 119.63, 118.44, 118.05, 114.82, 111.01, 109.67, 107.56, 58.97, 52.10 (2C), 49.83, 44.23, 32.67, 31.33 (2C). LC–MS (APCI<sup>+</sup>/ESI): found *m/z* = 504.2 [*M* + *H*]<sup>+</sup> (calcd. for C<sub>30</sub>H<sub>29</sub>N<sub>7</sub>O, 503.24). Purity: 97%, *t<sub>R</sub>* = 2.356 min.

**4-((2-((1-(4-(5-Methyl-1,2,4-oxadiazol-3-yl)phenethyl)piperidin-4-yl)amino)-1H-benzo[d]imidazol-1-yl) methyl) Benzonitrile (7).** Obtained from 5 (0.080 g, 0.24 mmol) and 2c (0.077 g, 0.29 mmol) as a pale-yellow solid (0.076 g, 61%); m.p.: 148–150 °C; *R<sub>f</sub>* (10% MeOH/DCM) 0.48. <sup>1</sup>H NMR (600 MHz, methanol-*d*<sub>4</sub>): δ 8.02 (d, *J* = 7.9 Hz, 2H), 7.70 (d, *J* = 8.0 Hz, 2H), 7.47 (d, *J* = 7.9 Hz, 2H), 7.41 (dd, *J* = 7.9, 0.9 Hz, 1H), 7.30 (d, *J* = 8.0 Hz, 2H), 7.17 (ddd, *J* = 7.9, 7.1, 1.0 Hz, 1H), 7.12 (dd, *J* = 8.0, 1.0 Hz, 1H), 7.08 (ddd, *J* = 8.0, 7.1, 1.0 Hz, 1H), 5.46 (s, 2H), 4.04 (tt, *J* = 10.5, 4.1 Hz, 1H), 3.75–3.63 (m, 2H), 3.44–3.38 (m, 2H), 3.26–3.18 (m, 2H), 3.18–3.12 (m, 2H), 2.65 (s, 3H), 2.40–2.31 (m, 2H), 1.99–1.89 (m, 2H). <sup>13</sup>C NMR (151 MHz, methanol-*d*<sub>4</sub>): δ 177.47, 167.78, 152.31, 141.41, 139.89, 132.95, 132.38 (2C), 129.12 (2C), 127.43 (2C), 127.07 (2C), 125.74, 122.33, 121.13, 119.23, 117.95, 114.13, 111.28, 108.49, 57.10, 51.63 (2C), 44.63, 30.15, 29.19 (2C), 29.09, 10.64. LC–MS (APCI<sup>+</sup>/ESI): found *m/z* = 518.2 [*M* + *H*]<sup>+</sup> (calcd. for C<sub>31</sub>H<sub>31</sub>N<sub>7</sub>O, 517.26). Purity: 97%, *t<sub>R</sub>* = 2.447 min.

***N*-(1-(4-(3-Methyl-1,2,4-oxadiazol-5-yl)phenethyl)piperidin-4-yl)-1H-benzo[d]imidazol-2-amine (15).** Obtained from 14a (0.85 g, 3.93 mmol) and 3d (1.35 g, 4.72 mmol) as a pale-yellow solid (1.18 g, 75%); m.p.: 171–173 °C; *R<sub>f</sub>* (10% MeOH/DCM), 0.20. <sup>1</sup>H NMR (400 MHz, methanol-*d*<sub>4</sub>): δ 8.04 (d, *J* = 8.3 Hz, 2H), 7.46 (d, *J* = 8.3 Hz, 2H), 7.20 (dd, *J* = 5.8, 3.2 Hz, 2H), 6.98 (dd, *J* = 5.8, 3.2 Hz, 2H), 3.69 (tt, *J* = 10.9, 4.3 Hz, 1H), 3.10–3.03 (m, 2H), 2.97–2.91 (m, 2H), 2.75–2.68 (m, 2H), 2.42 (s, 3H), 2.40–2.31 (m, 2H), 2.15–2.08 (m, 2H), 1.71–1.59 (m, 2H). <sup>13</sup>C NMR (101 MHz, methanol-*d*<sub>4</sub>): δ 176.08, 167.11, 154.29, 145.78, 137.16, 129.36 (2C), 127.75 (2C), 121.89, 120.10, 111.31, 59.21, 51.95 (2C), 49.33, 43.55, 32.72, 31.63 (2C), 9.99. LC–MS (APCI<sup>+</sup>/ESI): found *m/z* = 403.2 [*M* + *H*]<sup>+</sup> (calcd. for C<sub>23</sub>H<sub>26</sub>N<sub>6</sub>O, 402.22). Purity: 98%, *t<sub>R</sub>* = 2.469 min.

***N*-(1-(4-(3-(Trifluoromethyl)-1,2,4-oxadiazol-5-yl)phenethyl)piperidin-4-yl)-1H-benzo[d]imidazol-2-amine (23).** Obtained from



**14a** (0.250 g, 1.16 mmol) and **3e** (0.474 g, 1.39 mmol) as a white crystalline solid (0.290 g, 55%). m.p.: 102–104 °C;  $R_f$  (10% MeOH/DCM), 0.38.  $^1\text{H NMR}$  (600 MHz, methanol- $d_4$ ):  $\delta$  8.06 (d,  $J$  = 8.0 Hz, 2H), 7.48 (d,  $J$  = 8.0 Hz, 2H), 7.25 (dd,  $J$  = 5.8, 3.2 Hz, 2H), 7.05 (dd,  $J$  = 5.9, 3.1 Hz, 2H), 3.74 (tt,  $J$  = 10.5, 4.2 Hz, 1H), 3.21 (dt,  $J$  = 12.3, 4.0 Hz, 2H), 3.04–2.96 (m, 2H), 2.92–2.85 (m, 2H), 2.56 (td,  $J$  = 11.9, 2.7 Hz, 2H), 2.21–2.13 (m, 2H), 1.80–1.69 (m, 2H).  $^{13}\text{C NMR}$  (101 MHz, methanol- $d_4$ ):  $\delta$  169.05, 167.50, 153.15, 144.18, 135.53, 129.34 (2C), 127.50 (2C), 123.11, 120.87 (2C), 111.28 (2C), 58.70 (2C), 51.70, 49.10, 32.14, 30.94 (2C). LC–MS (APCI $^+$ /ESI): found  $m/z$  = 457.2 [M + H] $^+$  (calcd. for  $\text{C}_{23}\text{H}_{23}\text{F}_3\text{N}_6\text{O}$ , 456.19). Purity: 98%,  $t_R$  = 2.246 min.

**1-Methyl-N-(1-(4-(3-(trifluoromethyl)-1,2,4-oxadiazol-5-yl)phenethyl)piperidin-4-yl)-1H-benzod[imidazol-2-amine (24)**. Obtained from **14b** (0.150 g, 0.65 mmol) and **3e** (0.266 g, 0.78 mmol) as a white solid (0.202 g, 66%). m.p.: 90–92 °C;  $R_f$  (10% MeOH/DCM), 0.35.  $^1\text{H NMR}$  (600 MHz, methanol- $d_4$ ):  $\delta$  8.12 (d,  $J$  = 8.3 Hz, 2H), 7.56 (d,  $J$  = 8.3 Hz, 2H), 7.51–7.45 (m, 2H), 7.40–7.33 (m, 2H), 4.09–3.99 (m, 1H), 3.87–3.79 (m, 2H), 3.72 (s, 3H), 3.52–3.46 (m, 2H), 3.27–3.20 (m, 4H), 2.44–2.36 (m, 2H), 2.24–2.12 (m, 2H).  $^{13}\text{C NMR}$  (151 MHz, methanol- $d_4$ ):  $\delta$  168.88, 161.51, 149.24, 141.03, 131.40, 129.45 (2C), 128.97, 127.84 (2C), 124.01, 123.86, 123.70, 111.40, 109.61, 54.49 (2C), 42.38, 29.96, 28.28, 17.32, 15.90 (2C), 11.62. LC–MS (APCI $^+$ /ESI): found  $m/z$  = 471.2 [M + H] $^+$  (calcd. for  $\text{C}_{24}\text{H}_{25}\text{F}_3\text{N}_6\text{O}$ , 470.20). Purity: 99%,  $t_R$  = 2.375 min.

**(R)-4-((2-((1-(4-(3-Methyl-1,2,4-oxadiazol-5-yl)phenethyl)pyrrolidine-3-yl)amino)-1H-benzod[imidazol-1-yl)methyl] Benzonitrile (28)**. Obtained from **27a** (0.070 g, 0.22 mmol) and **3d** (0.075 g, 0.26 mmol) as a pale-yellow solid (0.087 g, 78%); m.p.: 74–76 °C;  $R_f$  (10% MeOH/DCM), 0.37.  $^1\text{H NMR}$  (600 MHz, methanol- $d_4$ ):  $\delta$  8.02 (d,  $J$  = 8.3 Hz, 2H), 7.66 (d,  $J$  = 8.4 Hz, 2H), 7.45 (d,  $J$  = 8.3 Hz, 2H), 7.33 (dd,  $J$  = 7.7, 1.1 Hz, 1H), 7.25 (d,  $J$  = 8.4 Hz, 2H), 7.06 (ddd,  $J$  = 7.7, 7.3, 1.0 Hz, 1H), 7.01 (dd,  $J$  = 8.0, 1.3 Hz, 1H), 6.96 (ddd,  $J$  = 8.0, 7.3, 1.1 Hz, 1H), 5.36 (s, 2H), 4.49 (tt,  $J$  = 6.8, 4.3 Hz, 1H), 2.99–2.89 (m, 4H), 2.86–2.74 (m, 3H), 2.59 (d,  $J$  = 6.8 Hz, 1H), 2.46–2.34 (m, 4H), 1.85–1.79 (m, 1H).  $^{13}\text{C NMR}$  (151 MHz, methanol- $d_4$ ):  $\delta$  175.43, 167.62, 154.06, 145.66, 142.19, 141.48, 133.92, 132.27 (2C), 129.32 (2C), 127.73 (2C), 127.13 (2C), 121.90, 121.34, 119.79, 118.01, 115.07, 111.06, 107.63, 60.32, 56.79, 52.70, 52.04, 44.32, 34.41, 31.40, 10.00. LC–MS (APCI $^+$ /ESI): found  $m/z$  = 504.2 [M + H] $^+$  (calcd. for  $\text{C}_{30}\text{H}_{29}\text{N}_7\text{O}$ , 503.24). Purity: 98%,  $t_R$  = 2.917 min. Specific rotation,  $[\alpha]_D^{25} = -4.59^\circ$ .

**Methyl 4-(2-(4-((1-Methyl-1H-benzod[imidazol-2-yl)amino]piperidin-1-yl)ethyl) Benzoate (32)**. Obtained from **14b** (5.00 g, 21.7 mmol) and **3f** (0.096 g, 6.37 mmol) as a cream white solid (5.78 g, 68%). m.p.: 148–149 °C;  $R_f$  (10% MeOH/DCM), 0.46.  $^1\text{H NMR}$  (400 MHz, methanol- $d_4$ ):  $\delta$  7.95 (d,  $J$  = 8.3 Hz, 2H), 7.37 (d,  $J$  = 8.3 Hz, 2H), 7.27 (dd,  $J$  = 7.4, 1.3 Hz, 1H), 7.13 (dd,  $J$  = 7.5, 1.6 Hz, 1H), 7.07–6.97 (m, 2H), 3.89 (s, 3H), 3.78 (tt,  $J$  = 11.2, 4.2 Hz, 1H), 3.52 (s, 3H), 3.15–3.06 (m, 2H), 2.96–2.88 (m, 2H), 2.72–2.65 (m, 2H), 2.32 (td,  $J$  = 12.1, 2.5 Hz, 2H), 2.17–2.09 (m, 2H), 1.69 (dtd,  $J$  = 12.2, 10.2, 3.8 Hz, 2H).  $^{13}\text{C NMR}$  (101 MHz, methanol- $d_4$ ):  $\delta$  167.16, 154.29, 145.88, 141.29, 134.58, 129.35 (2C), 128.57 (2C), 127.95, 120.69, 119.23, 114.39, 106.92, 59.43, 52.31 (2C), 51.11, 49.87, 32.76, 31.59 (2C), 27.16. LC–MS (APCI $^+$ /ESI): found  $m/z$  = 393.2 [M + H] $^+$  (calcd. for  $\text{C}_{23}\text{H}_{28}\text{N}_4\text{O}_2$ , 392.22). Purity: 98%,  $t_R$  = 0.422 min.

**1,5,6-Trimethyl-N-(1-(4-(3-methyl-1,2,4-oxadiazol-5-yl)phenethyl)piperidin-4-yl)-1H-benzod[imidazol-2-amine (61)**. Obtained from **60c** (0.080 g, 0.31 mmol) and **3d** (0.108 g, 0.37 mmol) as a light brown solid (0.066 g, 48%). m.p.: 120–122 °C;  $R_f$  (10% MeOH/DCM), 0.33.  $^1\text{H NMR}$  (400 MHz, methanol- $d_4$ ):  $\delta$  8.01 (d,  $J$  = 7.8 Hz, 2H), 7.39 (s, 1H), 7.31–7.18 (m, 3H), 3.85 (tt,  $J$  = 11.0, 4.2 Hz, 1H), 3.51 (s, 3H), 3.19–3.12 (m, 2H), 2.99–2.93 (m, 2H), 2.76–2.69 (m, 2H), 2.43 (s, 3H), 2.37–2.30 (m, 2H), 2.25 (s, 3H), 2.19 (s, 3H), 2.06–1.92 (m, 2H), 1.69–1.62 (m, 2H).  $^{13}\text{C NMR}$  (151 MHz, methanol- $d_4$ ):  $\delta$  176.22, 162.48, 141.73, 139.19, 137.65, 133.83, 132.01, 129.27, 128.76 (2C), 127.88 (2C), 119.19, 116.21, 108.54, 59.44, 56.56, 52.29 (2C), 34.92, 32.73, 31.66 (2C), 19.86, 19.72,

16.80. LC–MS (APCI $^+$ /ESI): found  $m/z$  = 445.3 [M + H] $^+$  (calcd. for  $\text{C}_{26}\text{H}_{32}\text{N}_6\text{O}$ , 444.26). Purity: 98%,  $t_R$  = 2.301 min.

**Methyl 1-Methyl-2-((1-(4-(3-methyl-1,2,4-oxadiazol-5-yl)phenethyl)piperidin-4-yl) amino)-1H-benzod[imidazole-5-carboxylate (68)**. Obtained from **60h** (0.200 g, 0.69 mmol) and **3d** (0.238 g, 0.83 mmol) as a white solid (0.255 g, 78%). m.p.: 98–99 °C;  $R_f$  (10% MeOH/DCM), 0.20.  $^1\text{H NMR}$  (400 MHz, methanol- $d_4$ ):  $\delta$  8.16 (d,  $J$  = 0.9 Hz, 1H), 8.02 (d,  $J$  = 7.9 Hz, 2H), 7.89 (dd,  $J$  = 7.8, 1.0 Hz, 1H), 7.58 (d,  $J$  = 7.8 Hz, 1H), 7.36 (d,  $J$  = 7.9 Hz, 2H), 3.89 (tt,  $J$  = 11.2, 4.5 Hz, 1H), 3.80 (s, 3H), 3.52 (s, 3H), 3.20–3.13 (m, 2H), 2.97–2.89 (m, 2H), 2.77–2.69 (m, 2H), 2.41 (s, 3H), 2.35–2.27 (m, 2H), 2.17–2.09 (m, 2H), 1.71–1.63 (m, 2H).  $^{13}\text{C NMR}$  (151 MHz, methanol- $d_4$ ):  $\delta$  175.90, 167.32, 162.30, 141.55, 139.12, 137.87, 133.64, 128.36 (2C), 127.96 (2C), 125.68, 124.34, 119.35, 116.64, 112.44, 59.51, 56.72, 52.95 (2C), 52.22, 34.72, 32.99, 31.77 (2C), 16.85. LC–MS (APCI $^+$ /ESI): found  $m/z$  = 475.2 [M + H] $^+$  (calcd. for  $\text{C}_{26}\text{H}_{30}\text{N}_6\text{O}_3$ , 474.24). Purity: 98%,  $t_R$  = 2.245 min.

**General Procedure 13: Synthesis of Compounds 18–22.** To a mixture of compound **15** (1.0 equiv), an appropriate alkyl bromide (1.2 equiv), and  $\text{K}_2\text{CO}_3$  (1.5 equiv) was added 5 mL DMF and the resulting solution was stirred under nitrogen at 70 °C for 12 h. Following completion, the reaction mixture was cooled to ambient temperature (23 °C) and diluted with EtOAc (25 mL). The resulting mixture was washed with  $\text{H}_2\text{O}$  (3  $\times$  30 mL), and then the combined aqueous layers were extracted with EtOAc (2  $\times$  20 mL). The EtOAc layers from both the wash and the extraction were combined and washed with 5% LiCl (2  $\times$  10 mL), followed by brine (15 mL), then dried over anhydrous  $\text{Na}_2\text{SO}_4$ , and concentrated *in vacuo*. The crude product was triturated with Et $_2$ O to obtain products. Further purification was performed by flash chromatography (4–8% MeOH/DCM) if required.

**1-(Cyclohexyl methyl)-N-(1-(4-(3-methyl-1,2,4-oxadiazol-5-yl)phenethyl) Piperidin-4-yl)-1H-benzod[imidazol-2-amine (18)**. Obtained from **15** (0.080 g, 0.20 mmol) and (bromomethyl)cyclohexane (0.043 g, 0.24 mmol) as a pale-yellow solid (0.080 g, 80%); m.p.: 78–80 °C;  $R_f$  (10% MeOH/DCM), 0.49.  $^1\text{H NMR}$  (600 MHz, methanol- $d_4$ ):  $\delta$  8.03 (d,  $J$  = 8.2 Hz, 2H), 7.46 (d,  $J$  = 8.2 Hz, 2H), 7.28 (dd,  $J$  = 7.7, 1.1 Hz, 1H), 7.11 (dd,  $J$  = 7.9, 1.3 Hz, 1H), 7.02 (ddd,  $J$  = 7.9, 7.2, 1.3 Hz, 1H), 6.98 (ddd,  $J$  = 7.7, 7.2, 1.3 Hz, 1H), 3.84 (d,  $J$  = 7.5 Hz, 2H), 3.81 (tt,  $J$  = 10.4, 4.0 Hz, 1H), 3.14–3.08 (m, 2H), 2.97–2.92 (m, 2H), 2.75–2.68 (m, 2H), 2.42 (s, 3H), 2.36–2.31 (m, 2H), 2.14–2.08 (m, 2H), 1.91–1.84 (m, 1H), 1.76–1.64 (m, 6H), 1.63–1.57 (m, 2H), 1.24–1.15 (m, 2H), 1.11–1.03 (m, 2H).  $^{13}\text{C NMR}$  (151 MHz, methanol- $d_4$ ):  $\delta$  176.35, 168.50, 154.86, 146.67, 141.92, 135.24, 130.27, 128.64, 125.33, 122.77, 121.54, 120.06, 115.27, 108.73, 60.14, 53.23 (2C), 50.89, 38.25, 33.62, 32.39 (2C), 31.14, 26.88 (2C), 26.36 (2C), 10.90. LC–MS (APCI $^+$ /ESI): found  $m/z$  = 499.3 [M + H] $^+$  (calcd. for  $\text{C}_{30}\text{H}_{38}\text{N}_6\text{O}$ , 498.31). Purity: 98%,  $t_R$  = 2.523 min.

**General Procedure 14: Synthesis of 1,2,4-Oxadiazoles (35–41) and Amides (43–51).** To a solution of **32** (4.00 g, 10.2 mmol) in MeOH (50 mL) was added 2 M aqueous KOH (25 mL, 51 mmol). The reaction mixture was stirred at 79 °C temperature for 2 h. After completion (monitored by TLC), MeOH was taken off *in vacuo* and the residue was diluted with  $\text{H}_2\text{O}$ . The solution was then acidified to pH 2 under ice with 3 M HCl, and the precipitate was filtered and recrystallized in MeOH to afford the carboxylic acid (**33**) product as an off-white solid quantitatively. A round-bottom flask containing **33** from the previous step (3.50 g, 9.26 mmol) was charged with thionyl chloride,  $\text{SOCl}_2$  (15 mL), and the resulting mixture was refluxed at 80 °C for 2 h. After completion, excess thionyl chloride was evaporated *in vacuo*, and the residue was taken up in 30 mL of toluene and evaporated *in vacuo* three (3) times to give acyl chloride **34** in quantitative yield.

An appropriate amine or amidoxime (**31**, 1.2 equiv) was added to a stirring solution containing acyl chloride **34** (0.060 g, 0.151 mmol) and Et $_3$ N (43  $\mu\text{L}$ , 0.303 mmol, 2.0 equiv) in 10 mL of dry THF. The resulting mixture was stirred at room temperature (20 °C) for 6–10 h. After completion, THF was evaporated *in vacuo*, and the residue was purified *via* column chromatography to afford amides (43–51)

and *O*-acylamidoximes. Each flask containing crude *O*-acylamidoximes was charged with  $K_2CO_3$  (0.042 g, 0.303 mmol, 2.0 equiv), and MeCN was added. The resulting solution was refluxed at 85 °C for 12 h. Upon completion, the mixture was filtered, and the solvent was taken off *in vacuo*. 1,2,4-Oxadiazoles (**35**–**41**) were obtained *via* column chromatography using 7–12% MeOH/DCM gradient as an eluent.

*N*-(1-(4-(3-Isopropyl-1,2,4-oxadiazol-5-yl)phenethyl)piperidin-4-yl)-1-methyl-1H-benzod[imidazol-2-amine (**35**). Obtained from **31a** (0.019 g, 0.18 mmol) as a light brown solid (0.041 g, 61% over two steps). m.p.: 135–137 °C;  $R_f$  (10% MeOH/DCM), 0.42.  $^1H$  NMR (600 MHz, methanol- $d_4$ ):  $\delta$  8.06 (d,  $J$  = 8.2 Hz, 2H), 7.53 (d,  $J$  = 8.2 Hz, 2H), 7.33 (dd,  $J$  = 7.6, 1.2 Hz, 1H), 7.11 (dd,  $J$  = 8.1, 1.2 Hz, 1H), 7.03 (ddd,  $J$  = 7.6, 7.2, 1.2 Hz, 1H), 6.97 (ddd,  $J$  = 8.1, 7.2, 1.2 Hz, 1H), 3.80 (tt,  $J$  = 10.9, 4.3 Hz, 1H), 3.52 (s, 3H), 3.21 (hept,  $J$  = 6.8 Hz, 1H), 3.09–3.02 (m, 2H), 2.99–2.89 (m, 2H), 2.75–2.67 (m, 2H), 2.36–2.24 (m, 2H), 2.19–2.08 (m, 2H), 1.76–1.62 (m, 2H), 1.22 (d,  $J$  = 6.8 Hz, 6H).  $^{13}C$  NMR (151 MHz, methanol- $d_4$ ):  $\delta$  175.44, 167.09, 155.33, 147.40, 141.09, 133.87, 130.69 (2C), 128.09 (2C), 121.88, 120.99, 120.08, 114.44, 107.28, 60.09, 54.11 (2C), 50.55, 39.85, 32.49, 31.89 (2C), 30.87, 28.76, 21.32 (2C). LC–MS (APCI<sup>+</sup>/ESI): found  $m/z$  = 445.2 [M + H]<sup>+</sup> (calcd. for  $C_{26}H_{32}N_6O$ , 444.26). Purity: 98%,  $t_R$  = 2.192 min.

*N*-(2-Hydroxyethyl)-4-(2-(4-((1-methyl-1H-benzod[imidazol-2-yl)amino]piperidin-1-yl)ethyl)benzamide (**43**). Obtained from 2-aminoethanol (0.011 g, 0.18 mmol) as an off-white solid (0.052 g, 82%). m.p.: 214–216 °C;  $R_f$  (10% MeOH/DCM), 0.15.  $^1H$  NMR (600 MHz, methanol- $d_4$ ):  $\delta$  7.90 (d,  $J$  = 7.9 Hz, 2H), 7.43 (d,  $J$  = 7.9 Hz, 2H), 7.21 (dd,  $J$  = 8.0, 1.1 Hz, 1H), 7.10 (dd,  $J$  = 7.8, 1.3 Hz, 1H), 6.96 (ddd,  $J$  = 8.0, 7.5, 1.3 Hz, 1H), 6.88 (ddd,  $J$  = 7.8, 7.5, 1.1 Hz, 1H), 4.19–4.12 (dd,  $J$  = 13.8, 6.9 Hz, 2H), 4.08–4.01 (m, 2H), 3.58 (tt,  $J$  = 10.8, 4.1 Hz, 1H), 3.52 (s, 3H), 3.18–3.10 (m, 2H), 2.84–2.78 (m, 2H), 2.70–2.62 (m, 2H), 2.35–2.28 (m, 2H), 2.16–2.06 (m, 2H), 1.73–1.64 (m, 2H).  $^{13}C$  NMR (151 MHz, methanol- $d_4$ ):  $\delta$  168.03, 142.87, 140.48, 138.03, 136.44, 130.28 (2C), 128.92 (2C), 123.00, 120.38, 119.33, 113.74, 105.81, 63.28, 62.44, 60.24, 52.48 (2C), 51.22, 42.87, 34.34, 30.19 (2C). LC–MS (APCI<sup>+</sup>/ESI): found  $m/z$  = 422.2 [M + H]<sup>+</sup> (calcd. for  $C_{24}H_{31}N_5O_2$ , 421.25). Purity: 99%,  $t_R$  = 0.138 min.

**General Procedure 14: Hydrolysis of Esters and Synthesis of Carboxylic Acids **42** and **69**.** To a solution of the ester in EtOH or MeOH was added 2 M aqueous KOH (10 equiv). The reaction mixture was stirred at 80 °C temperature for 2 h. After completion, EtOH or MeOH was taken off *in vacuo* and the residue was diluted with H<sub>2</sub>O. The solution was then acidified to pH 2 under ice with 3 N aqueous HCl, and the precipitate was filtered. The product was collected after recrystallization in EtOH.

5-(4-(2-(4-((1-Methyl-1H-benzod[imidazol-2-yl)amino]piperidin-1-yl)ethyl)phenyl)-1,2,4-oxadiazole-3-carboxylic Acid (**42**). Obtained from **41** (0.040 g, 0.084 mmol) in 5 mL EtOH as an off white crystalline solid (0.036 g, 96%). m.p.: 194–196 °C;  $R_f$  (10% MeOH/DCM), 0.05.  $^1H$  NMR (600 MHz, methanol- $d_4$ ):  $\delta$  8.03 (d,  $J$  = 8.1 Hz, 2H), 7.46 (d,  $J$  = 8.1 Hz, 2H), 7.24 (dd,  $J$  = 7.9, 1.3 Hz, 1H), 7.11 (dd,  $J$  = 8.0, 1.3 Hz, 1H), 6.97–6.83 (m, 2H), 3.82 (tt,  $J$  = 11.0, 4.4 Hz, 1H), 3.51 (s, 3H), 3.12–3.07 (m, 2H), 2.99–2.89 (m, 2H), 2.76–2.65 (m, 2H), 2.39–2.28 (m, 2H), 2.18–2.11 (m, 2H), 1.73–1.65 (m, 2H).  $^{13}C$  NMR (151 MHz, methanol- $d_4$ ):  $\delta$  176.09, 172.25, 169.36, 147.87, 140.33, 138.47, 134.98, 129.83 (2C), 127.22 (2C), 122.39, 120.19, 119.15, 113.88, 105.22, 60.29, 53.10 (2C), 51.51, 35.87, 34.12, 30.40 (2C). LC–MS (APCI<sup>+</sup>/ESI): found  $m/z$  = 447.2 [M + H]<sup>+</sup> (calcd. for  $C_{24}H_{26}N_6O_3$ , 446.21). Purity: 98%,  $t_R$  = 0.135 min.

1-Methyl-2-((1-(4-(3-methyl-1,2,4-oxadiazol-5-yl)phenethyl)piperidin-4-yl)amino)-1H-benzod[imidazol-5-carboxylic Acid (**69**). Obtained from **68** (0.200 g, 0.42 mmol) in 10 mL of MeOH as an off white solid (0.181 g, 94%). m.p.: 134–136 °C;  $R_f$  (10% MeOH/DCM), 0.08.  $^1H$  NMR (400 MHz, methanol- $d_4$ ):  $\delta$  8.11 (d,  $J$  = 1.3 Hz, 1H), 8.01 (d,  $J$  = 8.0 Hz, 2H), 7.89 (dd,  $J$  = 7.8, 1.3 Hz, 1H), 7.58 (d,  $J$  = 7.8 Hz, 1H), 7.36 (d,  $J$  = 8.0 Hz, 2H), 3.87 (tt,  $J$  = 10.7, 4.0 Hz, 1H), 3.52 (s, 3H), 3.20–3.12 (m, 2H), 2.97–2.90 (m,

2H), 2.78–2.69 (m, 2H), 2.44 (s, 3H), 2.36–2.27 (m, 2H), 2.18–2.09 (m, 2H), 1.71–1.64 (m, 2H).  $^{13}C$  NMR (151 MHz, methanol- $d_4$ ):  $\delta$  175.87, 167.22, 161.89, 141.49, 139.19, 137.77, 133.78, 128.44 (2C), 127.10 (2C), 125.86, 124.13, 119.45, 116.48, 112.58, 56.98, 52.88 (2C), 52.29, 34.69, 33.01, 31.65 (2C), 16.98. LC–MS (APCI<sup>+</sup>/ESI): found  $m/z$  = 461.2 [M + H]<sup>+</sup> (calcd. for  $C_{25}H_{28}N_6O_3$ , 460.22). Purity: 96%,  $t_R$  = 0.135 min.

7-Nitro-*N*-(2-(2-((1-(4-(5-(trifluoromethyl)-1,2,4-oxadiazol-3-yl)phenethyl)piperidin-4-yl)amino)-1H-benzod[imidazol-1-yl)ethyl)benzo[*c*][1,2,5]oxadiazole-4-amine (**23-NBD**). A mixture amine **71** (0.150 g, 0.30 mmol) and NaHCO<sub>3</sub> (0.076 g, 0.90 mmol) in 5 mL of H<sub>2</sub>O was stirred at 65 °C for 10 min. A solution of 4-chloro-7-nitrobenzo[*c*][1,2,5]oxadiazole NBD-Cl (0.060 g, 0.30 mmol) in MeCN (5 mL) was then added to the heated mixture dropwise *via* a syringe. The resulting reaction mixture was stirred at 65 °C for 2 h, during which a gradual color change from yellow to dark brown was observed. After completion, the mixture was cooled and MeCN was removed *in vacuo*. The aqueous residue was then filtered and extracted with EtOAc (3 × 20 mL). Combined organic phases were washed with brine and dried over anhydrous Na<sub>2</sub>SO<sub>4</sub>. Column chromatography using 8–10% MeOH/DCM was performed to obtain the product as a blackish solid (0.145 g, 73%). m.p.: 53–54 °C.  $R_f$  (10% MeOH/DCM), 0.51.  $^1H$  NMR (600 MHz, DMSO- $d_6$ ):  $\delta$  8.67–8.60 (br-s, 2H), 8.47 (d,  $J$  = 8.7 Hz, 1H), 8.21 (d,  $J$  = 8.7 Hz, 1H), 8.04 (d,  $J$  = 7.9 Hz, 1H), 7.56 (d,  $J$  = 7.9 Hz, 1H), 7.36 (d,  $J$  = 7.5 Hz, 1H), 7.29–7.18 (m, 1H), 7.15–7.08 (m, 1H), 7.03–7.95 (m, 1H), 6.47 (d,  $J$  = 6.2 Hz, 1H), 4.58 (m, 2H), 4.13–4.08 (m, 1H), 3.99–3.83 (m, 2H), 3.77–3.62 (m, 4H), 3.29–3.16 (m, 4H), 2.38–1.97 (m, 4H). LC–MS (APCI<sup>+</sup>/ESI): found  $m/z$  = 663.2 [M + H]<sup>+</sup> (calcd. for  $C_{31}H_{29}F_3N_{10}O_4$ , 662.23). Purity: 98%,  $t_R$  = 2.658 min.

**Aqueous Solubility.** Solubility was measured from amorphous solid forms of the compounds using the turbidimetric method. Following the dissolution of test compound in DMSO to make a 10 mM stock solution, a pre-dilution plate was prepared by taking from each stock solution and serially diluting in triplicate to yield concentrations from 0.25 to 10.0 mM on a 96-well plate. From each pre-dilution solution, secondary dilutions of the compounds in both DMSO and 0.01 M pH 7.4 PBS were prepared in triplicate on a second 96-well plate. Wells in columns 1–6 would contain compounds in DMSO, while those in columns 7–12 would contain samples in PBS at similar nominal concentrations as those in DMSO. The final volume of solvent in each assay plate was 200  $\mu$ L, prepared by pipetting 4  $\mu$ L each of solution from the pre-dilution plate to the corresponding well into both DMSO and PBS (both 196  $\mu$ L). This ensures that the final concentration of DMSO in the PBS aqueous buffer does not exceed 2% v/v. Similarly, a second secondary plate containing compound concentrations of 60, 100, and 120  $\mu$ M was also prepared. Different concentrations in DMSO were prepared as controls to determine false turbidimetric absorbance readings arising from the compounds in solution absorbing incident radiation at the test wavelength. Following preparation, the assay plate was covered and left to equilibrate for 2 h at 25 °C. Afterward, UV–vis absorbance readings from the plate were measured at 620 nm using a SpectraMax 340PC<sup>384</sup> microplate reader. Plots of corrected absorbance against the compound concentration were computed for a graphical representation of the data using MS Excel. Reserpine and hydrocortisone were used as positive and negative controls, respectively.

**In Vitro Antiplasmodium Assay at UCT.** Compounds were tested using a parasite lactate dehydrogenase assay as a marker for parasite survival. Briefly, the respective stock solutions of CQ diphosphate and test compounds were prepared to 2 mg·mL<sup>-1</sup> in distilled water (for CQ) and 100% DMSO for test compounds and then stored at –20 °C, and further dilutions were prepared on the day of the experiment. The cultures were synchronized in the ring stage using 15 mL of 5% (w/v) D-sorbitol in water. Synchronous cultures of *Pf*NF54 (CQ-S) and *Pf*K1 (MDR) in the late trophozoite stage were prepared to 2% parasitemia and 2% hematocrit. Compounds were tested at starting concentrations of 10,000 ng·mL<sup>-1</sup> (1000 ng·mL<sup>-1</sup> for CQ), which were then serially diluted 2-fold in a complete medium to give 10 concentrations with a final volume of 200  $\mu$ L in each well.

Parasites were incubated in the presence of the compounds at 37 °C under hypoxic conditions (4% CO<sub>2</sub> and 3% O<sub>2</sub> in N<sub>2</sub>) for 72 h. After incubation, 100 μL of MalStat reagent and 15 μL of resuspended culture were combined followed by addition of 25 μL of nitro blue tetrazolium chloride. The plates were kept in the dark for 10 min in order to fully develop, after which absorbance was measured at 620 nm on a microplate reader. Raw data was processed using GraphPad Prism 4.0 (La Jolla, California, USA) to analyze the dose–response.

**In Vitro Antiplasmodium Assay at Swiss TPH.** The testing was performed with the modified [<sup>3</sup>H]-hypoxanthine incorporation assay, as previously reported.<sup>34</sup>

**In Vitro Cytotoxicity Assay.** Compounds were screened against CHO mammalian cell lines using the 3-(4,5-dimethylthiazol-2-yl)-2,5-diphenyltetrazoliumbromide (MTT) assay.<sup>35</sup> Emetine was used as the reference standard. It was prepared to 2 mg/mL in distilled water, while the stock solutions of test compounds were prepared to 20 mg/mL in DMSO (100%), with the highest concentration of solvent to which the cells were exposed having no measurable effect on the cell viability. The initial concentration of the compounds and control was 100 μg/mL, which was serially diluted in a complete medium with 10-fold dilutions to give six concentrations, the lowest being 0.001 μg/mL. Plates were incubated for 48 h with 100 μL of test compound and 100 μL of cell suspension in each well and developed afterward by adding 25 μL of sterile MTT (Thermo Fisher Scientific) to each well followed by 4 h of incubation in the dark. The plates were then centrifuged, the medium aspirated, and 100 μL of DMSO was added to dissolve crystals before reading the absorbance at 540 nm. Data were analyzed, and the sigmoidal dose–response was derived using GraphPad Prism version 4.0 software. All experiments were performed as three independent biological repeats, each with technical triplicate.

**In Vitro Metabolic Stability Assay.** This assay was performed in duplicate using a 96-well microtiter plate. Test compounds (0.1 μM) were incubated at 37 °C in mouse and pooled human liver microsomes with a final protein concentration of 0.4 mg·mL<sup>-1</sup>, XenoTech, Lenexa, KS suspended in 0.1 M phosphate buffer at pH 7.4 for predetermined time points. This was in the presence and absence of cofactor-reduced nicotinamide adenine dinucleotide phosphate (NADPH, 1.0 mM). The reactions were quenched by adding ice-cold MeCN containing an internal standard (carbamazepine, 0.0236 μg/mL). The samples were centrifuged, and the supernatant was analyzed via liquid chromatography–tandem mass spectrometry (LC–MS/MS) (Agilent Rapid Resolution HPLC, AB SCIEX 4500 MS). The relative loss of the parent compound with time was monitored, and plots were prepared for each compound of Ln% remaining versus time to determine the first-order rate constant for compound depletion. This was used to calculate the degradation half-life and subsequently to predict the *in vitro* intrinsic clearance (CL<sub>int</sub>) and *in vitro* hepatic extraction ratio (E<sub>H</sub>).<sup>36</sup>

**In Vivo Antiplasmodium Assay at Swiss TPH.** *In vivo* efficacy was assessed as previously described,<sup>37</sup> with the modification that mice (*n* = 3) were infected with a GFP-transfected *P. berghei* ANKA strain (donated by A. P. Waters and C. J. Janse, Leiden University, The Netherlands), and parasitemia was determined using standard flow cytometry techniques. The detection limit was 1 parasite in 1000 erythrocytes (that is, 0.1%). The activity was calculated as the difference between the mean percent parasitemia for the control and treated groups expressed as a percent relative to the control group. Compounds were dissolved or suspended in a vehicle consisting of 70% Tween-80 and 30% ethanol, followed by a 10-fold dilution in H<sub>2</sub>O and oral administration as four consecutive daily doses (4, 24, 48, and 72 h after infection). Blood samples for the quadruple-dose regimens were collected on day 4 (96 h after infection). The survival time in days was also recorded up to 30 days after infection. A compound was considered curative if the animal survived to day 30 after infection with no detectable parasites by slide reading.

*In vivo* studies conducted at the Swiss TPH, Basel were approved by the veterinary authorities of the Canton Basel-Stadt (permit nos. 1731 and 2303) based on Swiss Cantonal (Verordnung Veterinäramt

Basel-Stadt) and National Regulations (The Swiss Animal Protection Law, Tierschutzgesetz).

**Fluorescence Live-Cell Imaging.** A Nunc Lab-Tek II 8-well chamber slide (Thermo Fisher Scientific) with no. 1.5 cover glass was coated with a 150 μL poly-L-lysine solution for 10 min after which the excess solution was removed, and the chamber slide was air-dried. Five microliters of human erythrocytes infected with *P. falciparum* chloroquine-sensitive strain (NF54) were resuspended in 5 mL of Ringer's solution (pH 7.5). One hundred microliters of aliquot of the suspended cells was placed in each well of the chamber slide and incubated for 30 min to allow the cells to adhere to the glass chamber. Excess Ringer's solution was removed alongside all non-adhering parasitized red blood cells. The cells were washed twice with Ringer's solution after which a new solution containing the appropriate concentration of drugs and organelle markers was added. SIM-SR microscopy was performed using an Elyra 7 with Lattice SIM2. A Plan-Apochromat 63×/1.40 Oil DIC M27 objective lens was used to keep laser transmission as low as possible to prevent phototoxicity to the cells. Images were captured and processed using Zeiss ZEN software (Carl Zeiss Microscopy GmbH).

## ■ ASSOCIATED CONTENT

### SI Supporting Information

The Supporting Information is available free of charge at <https://pubs.acs.org/doi/10.1021/acs.jmedchem.2c01516>.

Characterization data for compounds not shown in the main manuscript and the following assay protocols: kinetic solubility assay, *in vitro* antiplasmodium assay, *in vitro* antigametocytic activity assay, *in vitro* liver-stage assay (*P. berghei*-sporozoite infection), *in vitro* hERG assay, *in vitro* β-hematin formation inhibition assay, *in vivo* antiplasmodium assay at Swiss TPH, dried blood spots PK analysis, parasite heme fractionation assay, and optical polarimetry; <sup>1</sup>H and <sup>13</sup>C NMR spectra of selected and key target compounds, and HPLC-MS (low resolution) spectra of key target compounds (PDF)

Molecular formula strings (CSV)

## ■ AUTHOR INFORMATION

### Corresponding Author

**Kelly Chibale** – Department of Chemistry, South African Medical Research Council Drug Discovery and Development Research Unit, and Institute of Infectious Disease and Molecular Medicine, University of Cape Town, Rondebosch 7701, South Africa; Drug Discovery and Development Centre (H3D), DMPK & Pharmacology, University of Cape Town, Observatory 7925, South Africa; [orcid.org/0000-0002-1327-4727](https://orcid.org/0000-0002-1327-4727); Phone: +27-21-6502553; Email: [Kelly.Chibale@uct.ac.za](mailto:Kelly.Chibale@uct.ac.za); Fax: +27-21-6505195

### Authors

**Dickson Mambwe** – Department of Chemistry, University of Cape Town, Rondebosch 7701, South Africa; [orcid.org/0000-0003-4910-4479](https://orcid.org/0000-0003-4910-4479)

**Constance M. Korkor** – Department of Chemistry, University of Cape Town, Rondebosch 7701, South Africa; [orcid.org/0000-0001-6925-8905](https://orcid.org/0000-0001-6925-8905)

**Amanda Mabhula** – Drug Discovery and Development Centre (H3D), DMPK & Pharmacology, University of Cape Town, Observatory 7925, South Africa

**Zama Ngqumba** – Drug Discovery and Development Centre (H3D), DMPK & Pharmacology, University of Cape Town, Observatory 7925, South Africa

**Cleavon Cloete** – Drug Discovery and Development Centre (H3D), DMPK & Pharmacology, University of Cape Town, Observatory 7925, South Africa

**Malkeet Kumar** – Department of Chemistry, University of Cape Town, Rondebosch 7701, South Africa

**Paula Ladeia Barros** – Centro de Pesquisas Gonçalo Moniz, Fundação Oswaldo Cruz (Fiocruz), Instituto Gonçalo Moniz, CEP 40296-710 Salvador, Brazil

**Meta Leshabane** – Department of Biochemistry, Genetics & Microbiology, Institute for Sustainable Malaria Control, University of Pretoria, 0028 Pretoria, South Africa

**Dina Coertzen** – Department of Biochemistry, Genetics & Microbiology, Institute for Sustainable Malaria Control, University of Pretoria, 0028 Pretoria, South Africa

**Dale Taylor** – Drug Discovery and Development Centre (H3D), DMPK & Pharmacology, University of Cape Town, Observatory 7925, South Africa

**Liezl Gibbard** – Drug Discovery and Development Centre (H3D), DMPK & Pharmacology, University of Cape Town, Observatory 7925, South Africa

**Mathew Njoroge** – Drug Discovery and Development Centre (H3D), DMPK & Pharmacology, University of Cape Town, Observatory 7925, South Africa

**Nina Lawrence** – Drug Discovery and Development Centre (H3D), DMPK & Pharmacology, University of Cape Town, Observatory 7925, South Africa

**Janette Reader** – Department of Biochemistry, Genetics & Microbiology, Institute for Sustainable Malaria Control, University of Pretoria, 0028 Pretoria, South Africa

**Diogo Rodrigo Moreira** – Centro de Pesquisas Gonçalo Moniz, Fundação Oswaldo Cruz (Fiocruz), Instituto Gonçalo Moniz, CEP 40296-710 Salvador, Brazil; [orcid.org/0000-0003-3323-4404](https://orcid.org/0000-0003-3323-4404)

**Lyn-Marie Birkholtz** – Department of Biochemistry, Genetics & Microbiology, Institute for Sustainable Malaria Control, University of Pretoria, 0028 Pretoria, South Africa

**Sergio Wittlin** – Swiss Tropical and Public Health Institute, 4002 Basel, Switzerland; University of Basel, 4003 Basel, Switzerland; [orcid.org/0000-0002-0811-0912](https://orcid.org/0000-0002-0811-0912)

**Timothy J. Egan** – Department of Chemistry and Institute of Infectious Disease and Molecular Medicine, University of Cape Town, Rondebosch 7701, South Africa; [orcid.org/0000-0001-7720-8473](https://orcid.org/0000-0001-7720-8473)

Complete contact information is available at: <https://pubs.acs.org/10.1021/acs.jmedchem.2c01516>

## Notes

The authors declare no competing financial interest.

## ACKNOWLEDGMENTS

Christoph Fischli and Ursula Lehmann at Swiss TPH for performing *in vitro* and *in vivo* antimalarial efficacy studies, respectively, are appreciated. The Parasitology and DMPK teams at H3D are acknowledged. University of Cape Town, South African Medical Research Council (K.C., T.J.E. and L.-M.B.) and the South African Research Chairs Initiative of the Department of Science and Innovation administered through the South African National Research Foundation are greatly appreciated and acknowledged for their support (K.C.).

## ABBREVIATIONS

ACT, artemisinin combination therapy; AST, astemizole; AQ, amodiaquine; CDI, carbonyldiimidazole; CHO, Chinese hamster ovarian; CQ, chloroquine; DCC, N,N'-Dicyclohexylcarbodiimide; DMAP, 4-Dimethylaminopyridine; DMAST, desmethylastemizole; DMF, N,N-dimethylformamide; EDCI, 1-ethyl-3-(3-dimethylaminopropyl)carbodiimide;  $E_{H}$ , extraction ratio; hERG, human *ether-a-go-go*-related gene;  $IC_{50}$ , concentration of a drug that is required for 50% inhibition *in vitro*;  $I_{Kv}$ , potassium ion current; m.p., melting point; MSD, mean survival days; *P. berghei*, *Plasmodium berghei*; *P. falciparum*, *Plasmodium falciparum*; PK, pharmacokinetics; PTSA, *para*-toluene sulfonic acid;  $R_f$ , retardation factor; SAR, structure–activity relationship; SI, selectivity index; TCDD, 1,1'-thiocarbonyldiimidazole; TFA, trifluoroacetic acid anhydride;  $t_R$ , retention time.

## REFERENCES

- (1) Collins, F. H.; Paskewitz, S. M. Malaria: Current and Future Prospects for Control. *Annu. Rev. Entomol.* **1995**, *40*, 195–219.
- (2) World Health Organization. *World Malaria Report 2020*; Geneva, 2020.
- (3) Arie, F.; Witkowski, B.; Amaratunga, C.; Beghain, J.; Langlois, A.-C.; Khim, N.; Kim, S.; Duru, V.; Bouchier, C.; Ma, L.; et al. A Molecular Marker of Artemisinin-Resistant *Plasmodium Falciparum* Malaria. *Nature* **2014**, *505*, 50–55.
- (4) Uwimana, A.; Umulisa, N.; Venkatesan, M.; Svigel, S. S.; Zhou, Z.; Munyaneza, T.; Habimana, R. M.; Rucogoza, A.; Moriarty, L. F.; Sandford, R. Association of *Plasmodium Falciparum* Kelch13 R561H Genotypes with Delayed Parasite Clearance in Rwanda: An Open-Label, Single-Arm, Multicentre, Therapeutic Efficacy Study. *Lancet Infect. Dis.* **2021**, *21*, 1120–1128.
- (5) Zhou, Z.; Vorperian, V. R.; Gong, Q.; Zhang, S.; January, C. T. Block of HERG Potassium Channels by the Antihistamine Astemizole and Its Metabolites Desmethylastemizole and Norastemizole. *J. Cardiovasc. Electrophysiol.* **1999**, *10*, 836–843.
- (6) Suessbrich, H.; Waldegger, S.; Lang, F.; Busch, A. E. Blockade of HERG Channels Expressed in *Xenopus Oocytes* by the Histamine Receptor Antagonists Terfenadine and Astemizole. *FEBS Lett.* **1996**, *385*, 77–80.
- (7) Chong, C. R.; Chen, X.; Shi, L.; Liu, J. O.; Sullivan, D. J. A Clinical Drug Library Screen Identifies Astemizole as an Antimalarial Agent. *Nat. Chem. Biol.* **2006**, *2*, 415–416.
- (8) Musonda, C. C.; Whitlock, G. A.; Witty, M. J.; Brun, R.; Kaiser, M. Chloroquine–Astemizole Hybrids with Potent *In Vitro* and *In Vivo* Antiplasmodial Activity. *Bioorg. Med. Chem. Lett.* **2009**, *19*, 481–484.
- (9) Roman, G.; Crandall, I. E.; Szarek, W. A. Synthesis and Antiplasmodium Activity of Benzimidazole Analogues Structurally Related to Astemizole. *ChemMedChem* **2013**, *8*, 1795–1804.
- (10) Tian, J.; Vandermosten, L.; Peigneur, S.; Moreels, L.; Rozenski, J.; Tytgat, J.; Herdewijn, P.; Van den Steen, P. E.; De Jonghe, S. Astemizole Analogues with Reduced HERG Inhibition as Potent Antimalarial Compounds. *Bioorg. Med. Chem.* **2017**, *25*, 6332–6344.
- (11) Kumar, M.; Okombo, J.; Mambwe, D.; Taylor, D.; Lawrence, N.; Reader, J.; van der Watt, M.; Fontinha, D.; Sanches-Vaz, M.; Bezuidenhout, B. C.; et al. Multistage Antiplasmodium Activity of Astemizole Analogues and Inhibition of Hemozoin Formation as a Contributor to Their Mode of Action. *ACS Infect. Dis.* **2019**, *5*, 303–315.
- (12) Mambwe, D.; Kumar, M.; Ferger, R.; Taylor, D.; Njoroge, M.; Coertzen, D.; Reader, J.; van der Watt, M.; Birkholtz, L.-M.; Chibale, K. Structure–Activity Relationship Studies Reveal New Astemizole Analogues Active against *Plasmodium Falciparum* *In Vitro*. *ACS Med. Chem. Lett.* **2021**, *12*, 1333–1341.
- (13) Lassalas, P.; Gay, B.; Lasfargeas, C.; James, M. J.; Tran, V.; Vijayendran, K. G.; Brunden, K. R.; Kozlowski, M. C.; Thomas, C. J.;

Smith, A. B.; Huryn, D. M.; Ballatore, C. Structure Property Relationships of Carboxylic Acid Isosteres. *J. Med. Chem.* **2016**, *59*, 3183–3203.

(14) van der Westhuyzen, R.; Winks, S.; Wilson, C. R.; Boyle, G. A.; Gessner, R. K.; Soares de Melo, C.; Taylor, D.; de Kock, C.; Njoroge, M.; Brunschwig, C.; Lawrence, N.; Rao, S. P. S.; Sirgel, F.; van Helden, P.; Seldon, R.; Moosa, A.; Warner, D. F.; Arista, L.; Manjunatha, U. H.; Smith, P. W.; Street, L. J.; Chibale, K. Pyrrolo[3,4-c]pyridine-1,3(2H)-Diones: A Novel Antimycobacterial Class Targeting Mycobacterial Respiration. *J. Med. Chem.* **2015**, *58*, 9371–9381.

(15) Lee, S.; Yi, K. Y.; Yoo, S. E. Introduction of Heterocycles at the 2-Position of Indoline as Ester Bioisosteres. *Bull. Korean Chem. Soc.* **2004**, *25*, 207–212.

(16) Murarka, S.; Martín-Gago, P.; Schultz-Fademrecht, C.; Al Saabi, A.; Baumann, M.; Fansa, E. K.; Ismail, S.; Nussbaumer, P.; Wittinghofer, A.; Waldmann, H. Development of Pyridazinone Chemotypes Targeting the PDE $\delta$  Prenyl Binding Site. *Chem. - A Eur. J.* **2017**, *23*, 6083–6093.

(17) Maharvi, G. M.; Fauq, A. H. A Synthesis of the  $\gamma$ -Secretase Inhibitor BMS-708163. *Tetrahedron Lett.* **2010**, *51*, 6542–6544.

(18) Pankrat'eva, V. E.; Sharonova, T. V.; Tarasenko, M. V.; Baikov, S. V.; Kofanov, E. R. One-Pot Synthesis of 3,5-Disubstituted 1,2,4-Oxadiazoles Using Catalytic System NaOH–DMSO. *Russ. J. Org. Chem.* **2018**, *54*, 1250–1255.

(19) Kumar, N. N. B.; Kuznetsov, D. M.; Kutateladze, A. G. Intramolecular Cycloadditions of Photogenerated Azaxylenes with Oxadiazoles Provide Direct Access to Versatile Polyheterocyclic Ketopiperazines Containing a Spiro-Oxirane Moiety. *Org. Lett.* **2015**, *17*, 438–441.

(20) Presser, A.; Hüfner, A. Trimethylsilyldiazomethane ? A Mild and Efficient Reagent for the Methylation of Carboxylic Acids and Alcohols in Natural Products. *Monatshefte für Chemie/Chemical Mon.* **2004**, *135*, 1015–1022.

(21) Pitasse-Santos, P.; Sueth-Santiago, V.; Lima, M. 1,2,4- and 1,3,4-Oxadiazoles as Scaffolds in the Development of Antiparasitic Agents. *J. Braz. Chem. Soc.* **2017**, *29*, 435–456.

(22) Headley, A. D.; Ganesan, R.; Nam, J. The Effect of the Cyclopropyl Group on the Conformation of Chemotactic Formyl Tripeptides. *Bioorg. Chem.* **2003**, *31*, 99–108.

(23) deGrip, W. J.; Bovee-Geurts, P. H. M.; Wang, Y.; Verhoeven, M. A.; Lugtenburg, J. Cyclopropyl and Isopropyl Derivatives of 11-Cis and 9-Cis Retinals at C-9 and C-13: Subtle Steric Differences with Major Effects on Ligand Efficacy in Rhodopsin. *J. Nat. Prod.* **2011**, *74*, 383–390.

(24) Obach, R. S. Prediction of Human Clearance of Twenty-Nine Drugs from Hepatic Microsomal Intrinsic Clearance Data: An Examination of in Vitro Half-Life Approach and Nonspecific Binding to Microsomes. *Drug Metab. Dispos.* **1999**, *27*, 1350–1359.

(25) Olliaro, P.; Wells, T. N. C. The Global Portfolio of New Antimalarial Medicines Under Development. *Nature* **2009**, *85*, 584–595.

(26) Derbyshire, E. R.; Prudêncio, M.; Mota, M. M.; Clardy, J. Liver-Stage Malaria Parasites Vulnerable to Diverse Chemical Scaffolds. *Proc. Natl. Acad. Sci.* **2012**, *109*, 8511–8516.

(27) Lavis, L. D.; Raines, R. T. Bright Ideas for Chemical Biology. *ACS Chem. Biol.* **2008**, *3*, 142–155.

(28) Woodland, J. G. *Insights into the Mechanism of Action of Quinoline Antimalarials against Plasmodium Falciparum Revealed by Novel Fluorescent Analogues and Chemical Proteomics*, University of Cape Town, 2016.

(29) Maier, O.; Oberle, V.; Hoekstra, D. Fluorescent Lipid Probes: Some Properties and Applications (a Review). *Chem. Phys. Lipids* **2002**, *116*, 3–18.

(30) Edward, R. Use of DNA-Specific Anthraquinone Dyes to Directly Reveal Cytoplasmic and Nuclear Boundaries in Live and Fixed Cells. *Mol. Cells* **2009**, *27*, 391–396.

(31) Fitch, C. D.; Cai, G.; Chen, Y.-F.; Shoemaker, J. D. Involvement of Lipids in Ferriprotoporphyrin IX Polymerization in Malaria. *Biochim. Biophys. Acta - Mol. Basis Dis.* **1999**, *1454*, 31–37.

(32) Srivastava, I. K.; Vaidya, A. B. A Mechanism for the Synergistic Antimalarial Action of Atovaquone and Proguanil. *Antimicrob. Agents Chemother.* **1999**, *43*, 1334–1339.

(33) Ncokazi, K. K.; Egan, T. J. A Colorimetric High-Throughput  $\beta$ -Hematin Inhibition Screening Assay for Use in the Search for Antimalarial Compounds. *Anal. Biochem.* **2005**, *338*, 306–319.

(34) Snyder, C.; Chollet, J.; Santo-Tomas, J.; Scheurer, C.; Wittlin, S. In Vitro and in Vivo Interaction of Synthetic Peroxide RBx11160 (OZ277) with Piperaquine in Plasmodium Models. *Exp. Parasitol.* **2007**, *115*, 296–300.

(35) Liu, Y.; Peterson, D. A.; Kimura, H.; Schubert, D. Mechanism of Cellular 3-(4,5-Dimethylthiazol-2-Yl)-2,5-Diphenyltetrazolium Bromide (MTT) Reduction. *J. Neurochem.* **1997**, *69*, 581–593.

(36) Bertrand, M.; Jackson, P.; Walther, B. Rapid Assessment of Drug Metabolism in the Drug Discovery Process. *Eur. J. Pharm. Sci.* **2000**, *11*, S61–S72.

(37) González Cabrera, D.; Douelle, F.; Younis, Y.; Feng, T.-S.; Le Manach, C.; Nchinda, A. T.; Street, L. J.; Scheurer, C.; Kamber, J.; White, K. L.; et al. Structure–Activity Relationship Studies of Orally Active Antimalarial 3,5-Substituted 2-Aminopyridines. *J. Med. Chem.* **2012**, *55*, 11022–11030.

## Recommended by ACS

### Fragment Hopping-Based Design of Novel Biphenyl-DAPY Derivatives as Potent Non-Nucleoside Reverse Transcriptase Inhibitors Featuring Significantly Improved Anti-Resistan...

Ya-Li Sang, Fen-Er Chen, *et al.*

MARCH 30, 2023

JOURNAL OF MEDICINAL CHEMISTRY

READ 

### Discovery of Novel Sesquiterpene Lactone Derivatives as Potent PKM2 Activators for the Treatment of Ulcerative Colitis

Ping Wang, Lihong Hu, *et al.*

APRIL 05, 2023

JOURNAL OF MEDICINAL CHEMISTRY

READ 

### Structural Determinants of Indole-2-carboxamides: Identification of Lead Acetamides with Pan Antimycobacterial Activity

Pankaj Bhattarai, E. Jeffrey North, *et al.*

DECEMBER 23, 2022

JOURNAL OF MEDICINAL CHEMISTRY

READ 

### Artefenomel Regioisomer RLA-3107 Is a Promising Lead for the Discovery of Next-Generation Endoperoxide Antimalarials

Brian R. Blank, Adam R. Renslo, *et al.*

APRIL 04, 2023

ACS MEDICINAL CHEMISTRY LETTERS

READ 